MCB
Journals.ASM.org

Transmembrane Adaptor Protein PAG/CBP Is Involved in both Positive and Negative Regulation of Mast Cell Signaling

Lubica Draberova,[a] Viktor Bugajev,[a] Lucie Potuckova,[a] Ivana Halova,[a] Monika Bambouskova,[a] Iva Polakovicova,[a] Ramnik J. Xavier,[b,c] Brian Seed,[b] Petr Draber[a]

Department of Signal Transduction, Institute of Molecular Genetics, Academy of Sciences of the Czech Republic, Prague, Czech Republic[a]; Center for Computational and Integrative Biology, Massachusetts General Hospital, Harvard Medical School, Boston, Massachusetts, USA[b]; Broad Institute of Harvard University and Massachusetts Institute of Technology, Cambridge, Massachusetts, USA[c]

The transmembrane adaptor protein PAG/CBP (here, PAG) is expressed in multiple cell types. Tyrosine-phosphorylated PAG serves as an anchor for C-terminal SRC kinase, an inhibitor of SRC-family kinases. The role of PAG as a negative regulator of immunoreceptor signaling has been examined in several model systems, but no functions *in vivo* have been determined. Here, we examined the activation of bone marrow-derived mast cells (BMMCs) with PAG knockout and PAG knockdown and the corresponding controls. Our data show that PAG-deficient BMMCs exhibit impaired antigen-induced degranulation, extracellular calcium uptake, tyrosine phosphorylation of several key signaling proteins (including the high-affinity IgE receptor subunits, spleen tyrosine kinase, and phospholipase C), production of several cytokines and chemokines, and chemotaxis. The enzymatic activities of the LYN and FYN kinases were increased in nonactivated cells, suggesting the involvement of a LYN- and/or a FYN-dependent negative regulatory loop. When BMMCs from PAG-knockout mice were activated via the KIT receptor, enhanced degranulation and tyrosine phosphorylation of the receptor were observed. *In vivo* experiments showed that PAG is a positive regulator of passive systemic anaphylaxis. The combined data indicate that PAG can function as both a positive and a negative regulator of mast cell signaling, depending upon the signaling pathway involved.

Mast cells are widely distributed in the body, where they play important roles in innate as well as adaptive immune responses (1). To fulfill their role in adaptive immune responses, the cells express the high-affinity IgE receptor FcεRI on their plasma membranes. Aggregation of this tetrameric immunoreceptor, αβγ2, induces cell signaling events leading to the release of preformed inflammatory mediators and the *de novo* synthesis and release of leukotrienes, cytokines, and chemokines. The first well-defined biochemical step after FcεRI triggering is tyrosine phosphorylation of the immunoreceptor tyrosine-based activation motifs in the cytoplasmic tail of the FcεRI β and γ subunits by the SRC family protein tyrosine kinase (PTK) LYN (2, 3). The phosphorylated β and γ subunits then serve as binding and activation sites for LYN kinase and spleen tyrosine kinase (SYK), respectively. These two enzymes, together with FYN and other kinases, then phosphorylate various adaptor proteins and enzymes with a variety of functions in signal transduction pathways. The exact molecular events preceding LYN-mediated tyrosine phosphorylation of the FcεRI β subunit are not clear, and several models have been proposed, including the transphosphorylation model (4), the lipid raft model (5), and the PTK-protein tyrosine phosphatase (PTP) interplay model (6).

Our previous study with murine bone marrow-derived mast cells (BMMCs) showed that FcεRI triggering induced transient hyperphosphorylation of LYN kinase on its C-terminal regulatory tyrosine (Tyr 487), leading to the formation of a closed inactive conformation where the SRC homology 2 (SH2) domain interacts with phospho-Tyr 487 and transiently decreases LYN enzymatic activity (7). This finding was surprising because in T cells the corresponding SRC family kinase (SFK), LCK, showed decreased tyrosine phosphorylation of the C-terminal regulatory tyrosine and enhanced enzymatic activity after activation through T cell immunoreceptors (8, 9). Phosphorylation of the C-terminal inhibitory tyrosine in SFKs is catalyzed by the C-terminal SRC kinase (CSK) (10), a cytoplasmic PTK that can be anchored through its SH2 domain to PAG (11), also termed CBP (12). PAG/CBP (here, PAG) is a ubiquitously expressed transmembrane adaptor protein containing a short extracellular domain, a transmembrane domain, and a long cytoplasmic tail with multiple tyrosine-based motifs. Phosphorylated Tyr 314 in mouse PAG has been shown to be essential for CSK binding. PAG also possesses two proline-rich sequences that serve as binding sites for proteins with SH3 domains and a C-terminal VTRL motif for interaction with the PDZ domain of the cytoskeletal linker ezrin/radixin/moesin-binding protein of 50 kDa (13). Similar to some other transmembrane adaptor proteins, such as the non-T cell activation linker and linker for activation of T cells (LAT), PAG has two conserved cysteine residues, located in the vicinity of the transmembrane domain, which are the subject of posttranslational palmitoylation and which contribute to the poor solubility of the proteins in nonionic detergents and their presumed localization in membrane microdomains called lipid rafts (14, 15).

PAG in resting T cells associates with FYN kinase, which constitutively phosphorylates PAG on Tyr 314 to create a docking site for the CSK SH2 domain. This binding brings CSK to the vicinity of its substrate, SFK LCK, and enhances CSK catalytic activity, leading to phosphorylation of the LCK-inhibitory C-terminal tyrosine. Upon T cell receptor activation, PAG is rapidly dephospho-

Received 25 July 2014 **Accepted** 13 September 2014
Published ahead of print 22 September 2014
Address correspondence to Petr Draber, draberpe@img.cas.cz.

doi:10.1128/MCB.00983-14

rylated, CSK is released from PAG, and LCK is dephosphorylated on its C-terminal tyrosine. This modification increases the activity of LCK, leading to increased tyrosine phosphorylation of T cell receptor subunits and other substrates. A negative regulatory role of PAG in T cell signaling was confirmed in experiments with PAG knockdowns (KDs) (16) but not with PAG knockouts (KOs) (17, 18), suggesting that developmental compensatory mechanisms are involved.

In mast cells, PAG is phosphorylated by LYN kinase instead of FYN kinase, and following FcεRI triggering, the decrease in PAG phosphorylation is replaced by an increase (19, 20). Overexpression of PAG has been reported to inhibit FcεRI-mediated degranulation in rat basophilic leukemia (RBL) cells (21). Further experiments showed that FcεRI activation of BMMCs from LYN-deficient mice resulted in enhanced degranulation, whereas FYN-deficient cells showed the opposite effect (22–24). This finding supports the concept that SFKs are tightly regulated in the course of mast cell activation and important differences exist between early regulatory events induced by engagement of the T cell receptors and FcεRI. The exact role of PAG in mast cell activation remains to be determined.

Herein we present data on FcεRI-mediated activation events in BMMCs derived from mice deficient in PAG (PAG-KO mice) and from the corresponding wild-type (WT) mice (PAG-WT mice). We also attempted to determine whether any differences in activation are detectable between BMMCs in which PAG is downregulated by RNA interference and the corresponding control cells. Furthermore, we examined the role of PAG in cells activated through another important mast cell surface receptor, KIT. The combined data indicate that PAG functions as a positive or negative regulator of mast cell signaling and that the specific effect depends on the particular signaling pathway. We also show that PAG-deficient mice have a distinct phenotype *in vivo*, as assessed by induction of a passive systemic anaphylaxis response.

MATERIALS AND METHODS

Mice and cells. Mice deficient in PAG were generated by use of a modified bacterial artificial chromosome technology as previously described (25, 26). Briefly, the bacterial artificial chromosome clones were electroporated into strain 129Sv/J embryonic stem cells. Targeting in clone 7 was confirmed by fluorescence *in situ* hybridization. PAG-KO mice derived from clone 7 were born in the expected Mendelian frequency and were healthy. Transgenic founders were backcrossed to C57BL/6 mice for more than eight generations. For experiments, PAG-KO mice were mated with C57BL/6 mice, and their F1 descendants were genotyped by PCR using the following primers: PAG 1 F (5′-GAC AGC ACA GGA AAG GCC AAG-3′), PAG 2 R (5′-GTG TCC ACC GGT CCC TTC TG-3′), and PAG ZEO R (5′-CCA GGG TGT TGT CCG GCA C-3′), giving PCR products of 498 and 390 bp for the WT and PAG-KO alleles, respectively. Bone marrow cells were isolated from the femurs and tibias of 6- to 8-week-old PAG-KO mice or their WT littermates (PAG-WT mice). All animal studies were performed in compliance with the *Guide for the Care and Use of Laboratory Animals* (27) and were approved by the Animal Care and Usage Committee of the Institute of Molecular Genetics. Cells were cultured in RPMI 1640 medium supplemented with 100 U/ml penicillin, 100 μg/ml streptomycin, 71 μM 2-mercaptoethanol, minimum essential medium (MEM) nonessential amino acids, 0.7 mM sodium pyruvate, 2.5 mM L-glutamine, 12 mM D-glucose, recombinant mouse stem cell factor (SCF; 20 ng/ml; PeproTech EC), mouse recombinant interleukin-3 (IL-3; 20 ng/ml; PeproTech EC), and 10% fetal calf serum (FCS).

Antibodies and reagents. The following monoclonal antibodies (MAbs) were used: anti-LAT (28), anti-LYN (29), anti-FcεRI β chain (30), trinitrophenol (TNP)-specific immunoglobulin E (IgE) (IGEL b4.1) (31), and anti-hypoxanthine guanine phosphoribosyltransferase (anti-HPRT; Santa Cruz Biotechnology Inc.). Antipaxillin was obtained from BD Transduction Laboratories. Polyclonal antibodies specific for LYN and LAT were prepared in the Department of Signal Transduction, Prague, Czech Republic, by immunization of rabbits with the corresponding recombinant proteins or their fragments (32). Rabbit anti-IgE was prepared by immunization with whole IGEL b4.1. Polyclonal antibodies specific for FYN, actin, phospholipase C γ1 (PLCγ1), PLCγ2, GRB2, CSK, KIT, STAT5, SHIP1, phospho-KIT (Y568/570), and phospho-focal adhesion kinase (phospho-FAK; Y925), as well as horseradish peroxidase (HRP)-conjugated donkey anti-goat IgG, goat anti-mouse IgG, and goat anti-rabbit IgG, were obtained from Santa Cruz Biotechnology Inc. Antibodies specific for phospho-SYK (Y525/Y526), phospho-STAT5 (Y694), phospho-SH2-containing inositol 5′-phosphatase 1 (SHIP1; Y1020), and the Myc tag were obtained from Cell Signaling. PAG-specific rabbit polyclonal antibody was from Exbio. HRP-conjugated antiphosphotyrosine MAb (PY-20) was obtained from BD Biosciences. Antibodies specific for tumor necrosis factor alpha (TNF-α), IL-6, and IL-13 were purchased from PeproTech EC. Anti-mouse FcεRI labeled with fluorescein isothiocyanate (FITC) and anti-mouse KIT–allophycocyanin (APC) conjugates were obtained from eBiosciences. ^{45}Ca (specific activity, 773 MBq/mg Ca^{2+}) and [γ-^{32}P]ATP (specific activity, 222 TBq/mmol) were purchased from the Institute of Isotopes Co., Ltd. (Budapest, Hungary). A donkey anti-rabbit IgG–Alexa Fluor 488 conjugate and thapsigargin were obtained from Invitrogen. Mowiol 4-88 mounting solution was from Merck. Colloidal gold nanoparticles (Au-NPs; diameter, 30 nm), consisting of approximately 2×10^{11} Au-NPs/ml, were obtained from BBInternational. All other reagents were from Sigma-Aldrich.

Lentivirus shRNA constructs and cell transduction. A set of four murine Pag1 (Swiss-Prot accession number Q3U1F9) short hairpin (shRNA) constructs based on the pLKO.1 vector (TRCN0000124814 [shRNA14], TRCN0000124815 [shRNA15], TRCN0000124816 [shRNA16], and TRCN0000124817 [shRNA17]) were obtained from Open Biosystems. Each of the Pag1 shRNA constructs (14 μg) was mixed with Opti-MEM (1 ml; Invitrogen), 21 μl of ViraPower lentiviral packaging mix (Invitrogen), and 82 μl of Lipofectamine 2000 (Invitrogen). The mixture was homogenized by vortexing for 10 s and then incubated at room temperature for 20 min before it was added to semiconfluent (70%) HEK-293FT packaging cells growing in 20 ml of freshly added Dulbecco's medium supplemented with antibiotic and 10% FCS in 150-cm^2 tissue culture flasks. Three days later, the viruses in the culture supernatant were concentrated by centrifugation at 25,000 rpm for 2 h using a JA-25.50 rotor (Beckman Coulter). The pellets were resuspended in 1 ml of culture medium and added to 29 ml of culture medium containing 5×10^7 BMMCs. After 2 days, the medium was changed to virus-free medium and the cells were cultured for an additional 2 days (recovery period). Stable selection was achieved by culturing the transduced cells for 1 week in the presence of puromycin (5 μg/ml). Cells were pooled and analyzed for PAG expression by immunoblotting. Cells with the highest reduction in the amount of PAG, obtained with shRNA14 and shRNA15, were used for further experiments. Cells transfected with empty pLKO.1 vector were used as negative controls. For rescue experiments, mouse Pag1 cDNA (RefSeq accession number BC145761; catalog number 40131064; Open Biosystems) was amplified using forward primer 5′-AAAGAATTCGCCG CCACCAT**GGGCCCTGCAGGAAGCGT**-3′ (the EcoRI restriction site is underlined, the coding sequence is in bold) and reverse primer 5′-TTTG TCGAC**GAGCCTGGTGACATCTCTGC**-3′ (the SalI restriction site is underlined, the coding sequence is in bold). The amplified DNA was cloned via the EcoRI and SalI restriction sites (upstream of Myc) into the pFLAG-CMV-5a expression vector (Sigma-Aldrich) modified to express the Myc tag (kindly provided by V. Korinek). The cassette encoding the Myc-tagged Pag1 sequence was then amplified with the same forward primer described above and reverse primer 5′-TTTGCGGCCGCTTA**CA GGTCCTCCTCTGAGA**-3′ (the NotI restriction site is underlined, the

coding sequence is in bold) and recloned via EcoRI and NotI restriction sites into the pCDH-CMV-MCS-EF1-Puro expression lentivector (pCDH; catalog number CD510B-1; System Biosciences). The construct was verified by DNA sequencing. Viruses with pCDH-Pag-myc or empty pCDH were produced as described above. Medium with virus (30 ml) was filtered through a 0.22-μm-pore-size filter and divided into two aliquots. The first aliquot was used to transduce the WT or PAG-KO BMMCs at day 0. The second aliquot was preserved at 4°C and used for the second transduction of the same cells at day 3. Stable selection was achieved by culturing the cells for 7 days in the presence of puromycin (2 μg/ml), added 5 days after the first transduction.

Flow cytometry. To determine the surface expression of FcεRI, cells were exposed to FITC-conjugated anti-FcεRI (1 μg/ml). The samples were evaluated by flow cytofluorometry using a FACSCalibur instrument (BD Biosciences). For rescue experiments, cells were sensitized with TNP-specific IgE for 20 h of incubation in culture medium without IL-3 and SCF. Then they were washed and activated by antigen (TNP-bovine serum albumin [BSA] conjugate; 15 to 25 mol of TNP/mol of BSA; 100 ng/ml) for 90 min and fixed in 4% paraformaldehyde for 10 min at 37°C. The cells were washed once in phosphate-buffered saline (PBS), and free binding sites were blocked with 5% normal donkey serum (Jackson ImmunoResearch Laboratories) in PBS. After washing, the cells were incubated for 45 min with anti-TNF antibody diluted 1:100 in PBS with 0.5% BSA. After repeated washing, the cells were incubated for 30 min with a secondary donkey anti-rabbit IgG–Alexa Fluor 488 antibody conjugate, washed, and analyzed by flow cytometry using an LSR II flow cytometer (Becton Dickinson). For analysis of peritoneal mast cells, mice were sacrificed and injected intraperitoneally with 5 ml of PBS supplemented with 1% FCS. The peritoneal cavity was gently massaged for 30 s, and the injected PBS with free peritoneal fluid cells was withdrawn. One milliliter of PBS with peritoneal cells was spun down (400 × *g*, 5 min), and the cells were washed in cold PBS and stained for FcεRI (as described above) or KIT using the anti-mouse KIT–APC conjugate.

Cell activation. Before the experiments, BMMCs were cultured for 48 h in medium without SCF, followed by incubation for 12 to 16 h in SCF- and IL-3-free medium supplemented with IgE (1 μg/ml). Sensitized cells were washed in buffered salt solution (BSS; 20 mM HEPES, pH 7.4, 135 mM NaCl, 5 mM KCl, 1.8 mM $CaCl_2$, 5.6 mM glucose, 1 mM $MgCl_2$, 0.1% BSA). To quantify degranulation, the cells (0.15×10^6) in 30-μl aliquots were transferred into the wells of a 96-well plate and challenged with 30 μl of antigen (TNP-BSA conjugate), thapsigargin, or SCF at the concentrations indicated in Results. The degree of degranulation was determined as the amount of β-glucuronidase released into the supernatant, as described previously (33). Briefly, 40-μl aliquots of the cell supernatants were mixed in white wells of a 96-well plate (Nunc) with 40 μl of β-glucuronidase substrate (40 μM 4-methylumbelliferyl-β-D-glucuronide hydrate). After incubation for 60 min at 37°C, the reaction was stopped by adding 200 μl of ice-cold 0.2 M glycine buffer, pH 10.0, and fluorescence was determined in an Infinite M200 microtiter plate reader (Tecan) with 355-nm excitation and 460-nm emission filters. The total content of the enzyme in the cells was evaluated by measuring the levels of enzyme in the supernatant from cells lysed in 1% Triton X-100.

Extracellular calcium uptake. Calcium uptake was determined by a modification of a previously described procedure (34). Briefly, IgE-sensitized BMMCs (2×10^6) were resuspended in 100 μl BSS-BSA with 1 mM Ca^{2+}, mixed with 100 μl of BSS-BSA supplemented with $^{45}Ca^{2+}$ and various concentrations of antigen or thapsigargin, and incubated for selected time intervals at 37°C. The reactions were terminated by placing the tubes on ice and then suspending 100-μl aliquots on the walls of microtest tubes to make them separated by air space from the 12% BSA in PBS (300 μl) at the bottoms. Cells with bound $^{45}Ca^{2+}$ were separated from free $^{45}Ca^{2+}$ by centrifugation through 12% BSA at 3,220 × *g* for 15 min at 4°C. The cell pellets were recovered by freezing the tubes and slicing off the tube bottoms, and the cell pellets were solubilized with 1 ml of 1% Triton X-100. The radioactivity was counted in 10 ml scintillation liquid (EcoLite; ICN Biomedicals) in a scintillation counter with QuantaSmart software (PerkinElmer).

Immunoprecipitation and immunoblotting. Cells were pelleted and solubilized in ice-cold lysis buffer for immunoprecipitation (25 mM Tris-HCl, pH 8.0, 140 mM NaCl, 1 mM Na_3VO_4, 2 mM EDTA, 1 μg/ml aprotinin, 1 μg/ml leupeptin, 1 mM phenylmethylsulfonyl fluoride) supplemented with 1% *n*-dodecyl-β-D-maltoside and 1% Nonidet P-40 (for most experiments), 0.2% Triton X-100 (for FcεRI immunoprecipitation), or 1% Brij 96 (for kinase assays). After incubation (30 min on ice), the lysates were spun down (16,000 × *g* for 5 min at 4°C) and postnuclear supernatants were immunoprecipitated with the corresponding antibodies prebound to UltraLink-immobilized protein A or G (Pierce, Thermo Scientific). The immunoprecipitates were size fractionated by sodium dodecyl sulfate-polyacrylamide gel electrophoresis (SDS-PAGE) and immunoblotted with phosphotyrosine-specific PY-20–HRP conjugate or with protein-specific antibodies, followed by HRP-conjugated anti-mouse or anti-rabbit IgG antibody. Some phosphorylated proteins were determined by direct immunoblotting with phosphoprotein-specific antibodies, followed by immunoblotting with the corresponding secondary HRP-conjugated anti-mouse or anti-rabbit IgG. The HRP signal was detected by chemiluminescence. Immunoblots were quantified by use of a luminescent image analyzer (LAS-3000; Fuji Photo Film Co., Tokyo, Japan) and further analyzed by Aida image analyzer software (Raytest). The amount of phosphorylated proteins was normalized to the amount of immunoprecipitated proteins after stripping off the membranes, followed by development with the corresponding antibodies. In some experiments, parallel immunoblots instead of stripped membranes were used.

Sucrose density gradient fractionation. Sucrose density gradient separations were performed as previously described (35), with some modifications. Briefly, BMMCs (30×10^6) were lysed with 0.8 ml ice-cold lysis buffer (20 mM Tris-HCl, pH 8.0, 100 mM NaCl, 10 mM EDTA, 1 mM Na_3VO_4, 10 mM glycerophosphate, 1 mM phenylmethylsulfonyl fluoride, 100× diluted protease inhibitor cocktail, 5 mM iodoacetamide) supplemented with 1% Brij 96. The lysates were homogenized by passing them 10 times through a 27-gauge needle and adjusted to 40% (wt/vol) using 80% stock sucrose in 25 mM Tris-HCl, pH 7.5, 125 mM NaCl, and 2 mM EDTA. The gradient was prepared by adding 0.5 ml 80% sucrose at the bottom of a polyallomer tube (11 by 60 mm; Beckman Instruments), followed by 1.5 ml of 40% sucrose containing the cell lysate, 2 ml of 30% sucrose, and 1 ml of 10% sucrose. The gradient was ultracentrifuged at 210,000 × *g* for 4 h at 4°C using an SW55 Ti rotor (Beckman Instruments), and 0.5-ml fractions were collected from the top.

Immunocomplex kinase assay. The *in vitro* kinase assays were performed as previously described (36), with some modifications. FcεRI, LYN, and FYN were immunoprecipitated from nonactivated or antigen-activated cells lysed in lysis buffer for immunoprecipitation. Proteins immobilized to antibody-armed protein A beads were washed with kinase buffer (25 mM HEPES–NaOH, pH 7.2, 3 mM $MnCl_2$, 0.1% Nonidet P-40, 100 mM Na_3VO_4, 20 mM $MgCl_2$) and then resuspended in 25 μl kinase buffer supplemented with 2.5 μCi (92.5 kBq) of [γ-^{32}P]ATP, 100 μM ATP, and 0.5 μg/μl of acid-denatured enolase as the exogenous substrate. After incubation for 30 min at 37°C, the immunoprecipitates were eluted from the beads with reducing 2×-concentrated SDS-PAGE sample buffer and boiled for 7 min. The ^{32}P-labeled proteins were size fractionated by SDS-PAGE, transferred to a nitrocellulose membrane, and visualized by autoradiography. Films were quantified with Aida image analyzer software.

Cytokine and chemokine detection. IgE-sensitized BMMCs were activated with different concentrations of antigen. One hour later, mRNA was extracted using a TurboCapture 96 mRNA kit (Qiagen). Single-stranded cDNA was synthesized with Moloney murine leukemia virus reverse transcriptase (Invitrogen) according to the manufacturer's instructions. Real-time PCR amplifications of cDNAs were performed in 10-μl reaction volumes of a quantitative PCR (qPCR) mix containing 1 M 1,2-propanediol, 0.2 M trehalose, and SYBR green 1 (37) in 384-well

plates sealed with LightCycler 480 sealing foil (Roche Diagnostics) and analyzed in a LightCycler 480 apparatus (Roche Diagnostics). The following primer sets (sense/antisense) were used for amplification of the different cDNA fragments (the sizes of the amplified fragments are indicated in parentheses): actin, 5′-GATCTGGCACCACACCTTCT-3′/5′-GGGGTG TTGAAGGTCTCAAA-3′ (138 bp); glyceraldehyde-3-phosphate dehydrogenase (GAPDH), 5′-AACTTTGGCATTGTGGAAGG-3′/5′-ATCCA CAGTCTTCTGGGTGG-3′ (69 bp); ubiquitin, 5′-ATGTGAAGGCCAA GATCCAG-3′/5′-TAATAGCCACCCCTCAGACG-3′ (160 bp); TNF-α, 5′-CCCTCACACTCAGATCATCTTCT-3′/5′-GCTACGACGTGGGCT ACAG-3′ (61 bp); IL-6, 5′-GAGGATACCACTCCCAACAGACC-3′/5′-AAGTGCATCATCGTTGTTCATACA-3′ (141 bp); IL-13, 5′-AGACCA GACTCCCCTGTGCA-3′/5′-TGGGTCCTGTAGATGGCATTG-3′ (123 bp); CCL3, 5′-CATCGTTGACTATTTTGAAACCAG-3′/5′-GCCGGTT TCTCTTAGTCAGGAA-3′ (72 bp); and CCL4, 5′-CTTGGAGTTGAAC TGAGCAGC-3′/5-AGAGGGGCAGGAAATCTGAA-3′ (126 bp). The following cycling conditions were used: 3 min at 95°C, followed by 50 cycles of 10 s at 95°C, 20 s at 60°C, and 20 s at 72°C. Threshold cycle (C_T) values were determined by automated threshold analysis of the cycler. The specificity of the PCR was evaluated by examining melting curves. The genes for actin, GAPDH, and ubiquitin were used as reference genes, and the expression levels of all mRNAs were normalized to the geometric mean level of expression of these genes. The relative increase in the expression level of a cytokine was normalized to the level of expression by nonactivated WT cells in each experiment.

For detection of cytokines, an immuno-PCR method was used as described previously (38). Briefly, anti-TNF-α (1 μg/ml), anti-IL-6 (2 μg/ml), or anti-IL-13 (1 μg/ml) in 100 mM borate buffer (pH 9.5) was dispensed in 50-μl aliquots into the wells of a real-time 96-well plate (Eppendorf). After overnight incubation at 4°C, each well was washed four times with 200 μl of Tris-buffered saline (10 mM Tris-HCl, pH 7.4, 150 mM NaCl) containing 0.05% Tween 20 (TBST), and the remaining binding sites were blocked by 2 h of incubation at 37°C with TBST supplemented with 2% BSA. After washing, 50 μl of serial dilutions (0.1 to 100 ng/ml) of recombinant TNF-α, IL-6, or IL-13 (all from PeproTech EC) or the tested samples diluted in PBS–1% BSA was added. The samples were incubated for 1 h at 37°C, and after washing with TBST, 50 μl of Au-NPs armed with thiolated DNA oligonucleotide template (5′-thiol modifier C6 S-S/18-atom hexa-ethyleneglycol spacer-CCTTGAACCT GTGCCATTTGAATATATTAAGACTATACGCGGGAACA-3′] and with the corresponding cytokine-specific antibody was applied into each well. The wells were incubated for 1 h at 37°C and washed with TBST and deionized water. Fifty-microliter aliquots of qPCR master mix solution (see above) supplemented with 60 nM oligonucleotide primers 5′-CCTTGAACCTGTGCC ATTTG-3′ and 5′-GTCCCTCCATCTTCCTACTGTTCCACATGTTC CCGCGTATAGTCTT-3′ were then dispensed into each well. The plates were sealed, and the amount of template DNA bound to antigen-anchored functionalized Au-NPs was evaluated by real-time PCR using a Realplex4 Mastercycler apparatus (Eppendorf) with the following cycling conditions: 2 min at 94°C, followed by 40 cycles of 20 s at 94°C, 20 s at 53°C, and 20 s at 72°C. For the calculation of TNF-α, IL-6, and IL-13 concentrations, the corresponding C_T values were substituted into the regression equations obtained from the calibration curves constructed from the concentration series of appropriate recombinant proteins.

Chemotaxis assay. Chemotaxis responses were assayed in 24-well Transwell chambers (Corning) with 8-μm-pore-size polycarbonate filters in the upper wells. Chemoattractants (antigen or SCF) in 0.6 ml chemotaxis medium (RPMI 1640 supplemented with 1% BSA and 20 mM HEPES, pH 7.4) were added to the lower wells. IgE-sensitized BMMCs (0.3×10^6 in 120 μl chemotactic medium) were added to the upper wells. Cells migrating into the lower wells during the 8 h of incubation (37°C, 5% CO_2) were counted using an Accuri C6 flow cytometer (BD Biosciences).

Confocal microscopy. BMMCs (3×10^5) were attached to fibronectin-coated multitest slides (MP Biomedicals). Cells were fixed with 4% paraformaldehyde for 15 min at room temperature and permeabilized in 0.3% Triton X-100 for 20 min. Free binding sites were blocked with 5% normal donkey serum, and the cells were stained with rabbit anti-Myc tag antibody, followed by labeling with secondary antibody (donkey anti-rabbit IgG–Alexa Fluor 488 conjugate). After 60 min, the cells were washed and mounted in Mowiol 4-88 mounting solution supplemented with Hoechst 33258 nucleic acid stain (1 μg/ml; Molecular Probes) to label the nuclei. Samples were examined with a confocal laser scanning microscope (Leica TCS SP5) equipped with a ×63 (numerical aperture, 1.4) oil immersion objective.

Passive systemic anaphylaxis. The systemic anaphylactic reaction is accompanied by the release of histamine from activated mast cells, leading to a decreased body temperature (39). The body temperature was measured with an accuracy of ±0.1°C using a VitalView data acquisition system with ER-4000 energizer receivers, G2 E-mitter transponders, and VitalView software (Mini Mitter). G2 probes were implanted intra-abdominally into mice while they were under systemic anesthesia with isoflurane (Abbott Laboratories). Monitoring of body temperature was initiated 9 days after the surgery. Mice aged 11 to 18 weeks were sensitized by tail vein injection of TNP-specific IgE (3 μg in 100 μl PBS per mouse), and 24 h later, anaphylaxis was induced by intravenous administration of antigen (500 μg in 100 μl PBS per mouse). The body temperature was recorded at 1-min intervals for at least 3 h after antigen challenge.

Serum IgE quantification. Ninety-six-well enzyme-linked immunosorbent assay plates (Nunc) were coated for 16 h at 4°C with rat antibody specific for mouse IgE (1 μg/ml in PBS; 50 μl/well; BD Biosciences). Wells were washed (four times with TBST) and blocked by incubation at 22°C with TBST–2% BSA. After 2 h, the plates were washed and incubated for 1 h at 22°C with various concentrations of mouse IgE standard (1.95 to 125 ng/ml in PBS–1% BSA; BD Biosciences) or mouse serum samples (diluted 1:5 in PBS–1% BSA). Then, the wells were washed and the captured IgE was detected with biotinylated rat anti-mouse IgE antibody (2 μg/ml in PBS–1% BSA; BD Bioscience), washed, and incubated for 30 min with streptavidin-HRP conjugate (diluted 1:1,000 in PBS–1% BSA; BD Biosciences). Peroxidase substrate solution (0.5 mg/ml *o*-phenylenediamine and 0.015% H_2O_2 in 0.1 M NaH_2PO_4, pH 6.0) was used for colorimetric reaction. The reaction was stopped by adding 50 μl of 4 M H_2SO_4, and the absorbance at 492 nm was determined using an Infinite M200 plate reader (Tecan).

Statistical analysis. The significance of intergroup differences was evaluated by Student's *t* test.

RESULTS

Positive regulatory role of PAG on antigen-induced degranulation. To examine the role of PAG in mast cell signaling, we isolated bone marrow cells from homozygous F1-descendant PAG-KO and PAG-WT mice and cultured them in the presence of IL-3 and SCF to obtain BMMCs. Cells with or without PAG exhibited comparable growth parameters under *in vitro* conditions (not shown), suggesting that PAG had no effect on the growth response of mast cells to IL-3 and SCF. The same PAG-WT BMMCs were used for the production of PAG-KD cells after transduction with lentiviral vectors containing PAG shRNA constructs based on a pLKO vector (shRNA14 to shRNA17), followed by selection in puromycin. PAG-WT BMMCs infected with empty lentiviral vector were used as a negative control (pLKO). PAG-KO and PAG-WT cells expressed comparable amounts of surface FcεRI, as detected by flow cytometry (Fig. 1A). Similarly, no difference in surface FcεRI was observed among various PAG-KD cells and controls (not shown). As expected, we found no detectable PAG in PAG-KO cells using immunoblotting with PAG-specific antibody (Fig. 1B). The amount of PAG in PAG-KD cells was substantially reduced compared to that in control (pLKO) cells. The strongest inhibition was observed in the cells infected with the shRNA14 and shRNA15

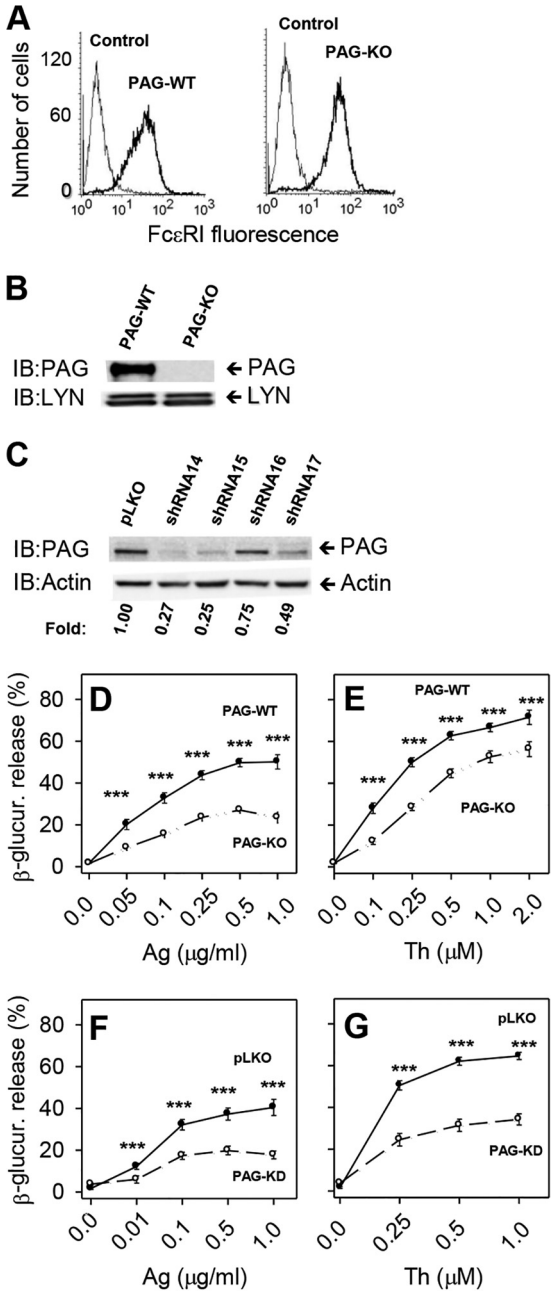

FIG 1 Positive regulatory role of PAG in antigen- or thapsigargin-induced degranulation. (A) BMMCs derived from WT mice (PAG-WT) or PAG-deficient mice (PAG-KO) were stained for surface FcεRI by use of an anti-FcεRI-FITC conjugate. Unstained WT cells were used as negative controls. Samples were analyzed by flow cytometry. (B, C) The presence of PAG in lysates from PAG-WT and PAG-KO BMMCs (B) or WT BMMCs infected with empty pLKO lentiviral vector (pLKO) or lentiviral vectors shRNA14 to shRNA17 (C) was determined by immunoblotting (IB). As loading controls, the membranes were also developed for LYN (B) or actin (C). The amount of PAG normalized to its amount in cells infected with the empty pLKO vector and actin loading control (fold) is also shown (C). For each panel, the results of one representative experiment out of a minimum of three performed are shown. (D, E) PAG-WT or PAG-KO BMMCs were sensitized (D) or not (E) with TNP-specific IgE (1 μg/ml) and then stimulated for 30 min with various concentrations of antigen (Ag) (D) or thapsigargin (Th) (E). (F, G) PAG-WT BMMCs were infected with empty pLKO lentiviral vector (pLKO) or with PAG shRNA14 and shRNA15 vectors (PAG-KD), and stable transfectants were activated with antigen (F) or thapsigargin (G), as described above. The amount of β-glucuronidase (β-glucur.) released from the cells was determined 30 min after triggering. Data represent means ± SEs calculated from 11 independent experiments performed in duplicate or triplicate in panels D and E and from 6 to 8 independent experiments performed in duplicate or triplicate in panels F and G. The statistical significance of differences between PAG-WT and PAG-KO cells or pLKO and PAG-KD cells is shown: ***, $P < 0.001$.

constructs, which reduced PAG expression by 73% and 75%, respectively (Fig. 1C). Infection with constructs containing shRNA16 and shRNA17 reduced PAG expression by 25% and 51%, respectively. Guided by these data, we used viruses containing shRNA14 and shRNA15 for further experiments with BMMCs. Because of the similar knockdown characteristics of these constructs, data from BMMCs infected with these shRNAs were combined and are presented under the common heading of PAG-KDs.

Using BMMCs with PAG-KO and PAG-KD and the corresponding controls, we first investigated whether PAG deficiency has any effect on mast cell degranulation after FcεRI triggering. Degranulation was estimated from the amount of β-glucuronidase released from activated cells. BMMCs were sensitized with TNP-specific IgE and then exposed to various concentrations of antigen. After 30 min, PAG-KO cells exhibited significantly lower levels of degranulation than WT cells at all concentrations of the antigen tested (0.05 to 1.0 μg/ml; Fig. 1D); the total amount of β-glucuronidase released from both cell types by Triton X-100 was similar (data not shown). These data indicate that the absence of PAG reduces antigen-induced degranulation but does not interfere with the production of β-glucuronidase in secretory vesicles. Significant inhibition of degranulation was also observed in PAG-KO cells activated with various concentrations of thapsigargin (0.1 to 2.0 μM; Fig. 1E). Thapsigargin induces the release of Ca^{2+} from intracellular stores by inhibiting the endoplasmic reticulum (ER) ATPase (40). The combined data suggest that PAG not only is involved in the CSK-mediated FcεRI-proximal regulation of SFKs but also could still have other functions distal to FcεRI regulation.

To test whether compensatory developmental alterations could be responsible for the unexpected properties of PAG-KO BMMCs, we examined antigen- and thapsigargin-induced degranulation in cells with PAG-KD and the corresponding controls. The data shown in Fig. 1F and G demonstrate that stimulation of PAG-KD cells with antigen or thapsigargin decreased the level of degranulation compared to that in the pLKO controls, supporting previous findings that PAG is a positive regulator of mast cell degranulation.

Positive regulatory role of PAG on Ca^{2+} response. Early events in mast cell signaling involve the release of Ca^{2+} from intracellular stores followed by the influx of extracellular Ca^{2+} through store-operated Ca^{2+} (SOC) channels in the plasma membrane (41). To determine whether PAG has a role in this process, we quantified Ca^{2+} uptake in PAG-deficient and control BMMCs. The data presented in Fig. 2A show that stimulation with antigen causes significantly lower levels of uptake of extracellular $^{45}Ca^{2+}$ in PAG-KO cells than in PAG-WT cells, reaching a peak at approximately 5 min after triggering in both cell types. Inhibition of Ca^{2+} uptake in PAG-KO cells was observed 5 min after triggering at all concentrations of the antigen tested (Fig. 2B). Significant inhibition of Ca^{2+} uptake in PAG-KO cells was also seen after stimulation for various time intervals (Fig. 2C) or with various

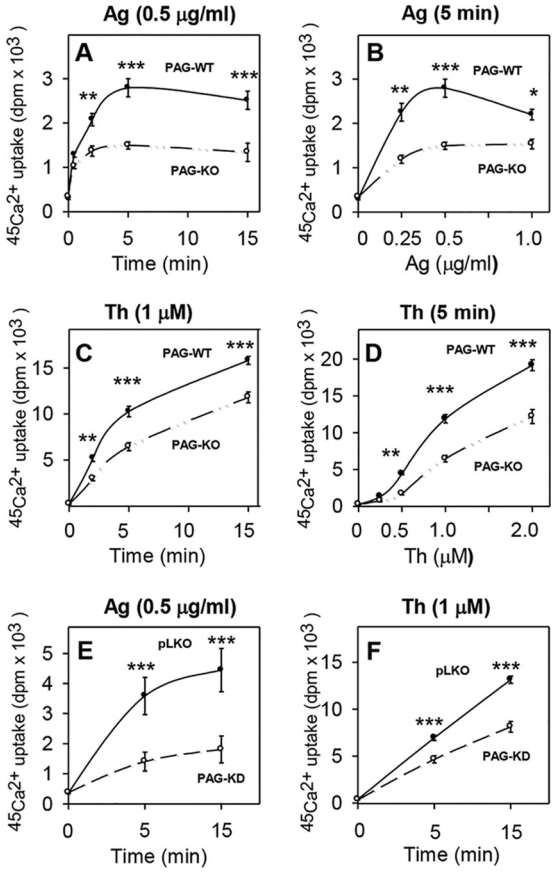

FIG 2 Positive regulatory role of PAG on antigen- or thapsigargin-induced calcium uptake. (A, B) PAG-WT and PAG-KO BMMCs were sensitized with IgE and then stimulated for various time intervals with antigen (0.5 μg/ml) (A) or with various concentrations of antigen for 5 min (B) in the presence of 1 mM extracellular $^{45}Ca^{2+}$. The reactions were terminated by centrifugation of the cells through a BSA gradient, and cell-bound radioactivity (in the sediment) was determined. (C, D) PAG-WT and PAG-KO BMMCs were activated for various time intervals with 1 μM thapsigargin (C) or with various concentrations of thapsigargin for 5 min (D), and the uptake of $^{45}Ca^{2+}$ was determined as described above. (E, F) PAG-WT BMMCs were infected with empty pLKO lentiviral vector (pLKO) or with PAG shRNA vectors (PAG-KD), and stable transfectants were activated with antigen (E) or thapsigargin (F) and analyzed as described above. Data represent means ± SEs from three to six independent experiments performed in duplicate or triplicate. *, $P < 0.05$; **, $P < 0.01$; ***, $P < 0.001$.

concentrations of thapsigargin (Fig. 2D). A positive regulatory role of PAG in calcium uptake after antigen (Fig. 2E) or thapsigargin (Fig. 2F) activation was also evident when PAG-KD cells were compared to the corresponding PAG-expressing (pLKO) controls. These data imply that the observed inhibition of degranulation in PAG-deficient cells could be at least in part attributable to decreased calcium mobilization.

Localization of CSK in lipid rafts depends on PAG. Previous studies localized PAG almost exclusively to lipid rafts, where it could interact with CSK and through this interaction negatively regulate lipid raft-associated SFKs (15). This conclusion was based on data evaluating the distribution of PAG in fractions after sucrose density gradient ultracentrifugation of lysates from cells disintegrated in nonionic detergents (11, 12) or 0.5 M $NaHCO_3$ (21). However, there are inconsistencies regarding the role of PAG in

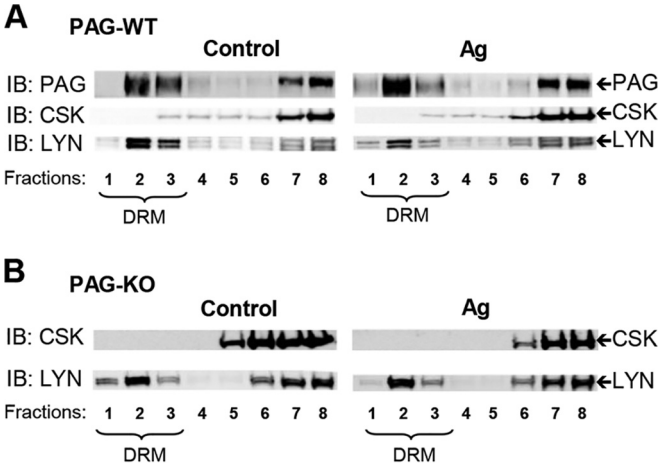

FIG 3 Localization of CSK in lipid rafts depends on PAG. IgE-sensitized PAG-WT BMMCs (A) or PAG-KO BMMCs (B) were nonactivated (Control) or activated for 5 min with antigen (250 ng/ml). After solubilization in lysis buffer containing 1% Brij 96, the whole-cell lysates were fractionated by sucrose density gradient ultracentrifugation as described in Materials and Methods. Individual fractions were collected and analyzed by immunoblotting for the presence of PAG, CSK, and LYN. Fractions containing DRMs are indicated. Representative data from three independent experiments are shown.

the localization of CSK in lipid rafts. One study found that the level of lipid raft-associated CSK in thymocytes was greatly reduced in the absence of PAG (18), whereas another concluded that PAG is dispensable for the localization of CSK in lipid rafts (17). To determine whether PAG contributes to the localization of CSK in lipid rafts in BMMCs, nonactivated or antigen-activated PAG-WT and PAG-KO BMMCs were solubilized in a buffer supplemented with 1% Brij 96 and fractionated by sucrose density gradient ultracentrifugation, and their presence in individual fractions was analyzed by immunoblotting. The distribution of LYN kinase, a well-known lipid raft marker in BMMCs, was also examined. In accordance with previous data (42), most of the LYN (88%) in nonactivated cells was associated with detergent-resistant membranes (DRM; fractions 1 to 3). Five minutes after activation with antigen, this amount was reduced by approximately half (Fig. 3A). In the same gradient fractions, less PAG was found in DRMs (55%), and no significant changes were observed after stimulation with antigen. Only a small fraction of CSK was found in DRM fractions (4%), and no significant changes were observed after activation with antigen. When lysates from PAG-KO BMMCs were analyzed, no CSK was found in DRM fractions from activated and nonactivated cells even after a longer exposure (Fig. 3B), suggesting that PAG is involved in the localization of CSK in DRMs.

PAG and tyrosine phosphorylation of signal transduction proteins. The first biochemically defined step after FcεRI triggering is tyrosine phosphorylation of the FcεRI subunits by SFK LYN, followed by engagement of other kinases and phosphorylation of a number of signal transduction proteins. To specify the role of PAG in these processes, we examined tyrosine phosphorylation of FcεRI and several selected proteins involved in early stages of antigen-induced mast cell signaling (SYK, LAT, extracellular signal-regulated kinase [ERK]) (43), as well as proteins involved in cell movement (FAK and paxillin) (44). In initial experiments, we looked for proteins phosphorylated on tyrosine in total cellular

lysates. We found that PAG-WT cells differed from PAG-KO cells in several tyrosine-phosphorylated proteins not only after antigen stimulation but also in the nonactivated state (Fig. 4A). Further analysis showed that FcεRI triggering caused an increase in tyrosine phosphorylation of FcεRI β and γ chains in WT cells and that this process was significantly reduced in PAG-KO cells (Fig. 4B). Tyrosine phosphorylation of SYK (Fig. 4C) and its substrates, LAT (Fig. 4D) and ERK (Fig. 4E), was also impaired in PAG-deficient cells. In contrast, FAK (Fig. 4F) and the focal adhesion-associated adaptor protein paxillin (Fig. 4G) showed elevated basal levels of tyrosine phosphorylation in PAG-KO cells; this difference was maintained after FcεRI triggering (Fig. 4F and G).

The observed decrease in tyrosine phosphorylation of FcεRI β and γ subunits in antigen-activated PAG-KO cells suggested an imbalance between PTKs and PTPs in the vicinity of the receptor. To examine FcεRI-associated PTK activity toward its endogenous substrate, FcεRI was immunoprecipitated from nonactivated and antigen-activated PAG-WT and PAG-KO cells, and the immunocomplexes were analyzed by *in vitro* kinase assays with [γ-^{32}P]ATP. Using PAG-WT cells, we observed a significant increase in radioactivity bound to FcεRI β and γ receptor subunits after activation with antigen (Fig. 5A and B). Surprisingly, when the receptor was precipitated from PAG-KO cells, strong phosphorylation of the receptor β and γ subunits was observed in nonactivated cells and was decreased after FcεRI triggering. These data, together with the results of immunoblotting experiments showing weak and comparable tyrosine phosphorylation of the β and γ subunits of FcεRI isolated from nonactivated PAG-WT and PAG-KO cells, suggest that the activity of PTKs bound to FcεRI isolated from PAG-KO cells is enhanced.

To determine the enzymatic activities of total LYN and FYN, the kinases were immunoprecipitated and their activities were assessed by an *in vitro* kinase assay. To overcome the problem with possible variation in the extent of nonphosphorylated residues in the target proteins, we used acid-denatured enolase as the exogenous substrate in immunocomplex kinase assays. The data in Fig. 5C to F show low but significantly higher levels of autophosphorylation of the LYN and FYN kinases immunoprecipitated from PAG-KO cells than of those immunoprecipitated from PAG-WT cells. Importantly, enolase phosphorylation was also enhanced in LYN and FYN immunoprecipitates obtained from PAG-KO cells. In contrast to the findings of previous studies (3, 19), we did not observe any increase in the activity of the kinases after FcεRI triggering, which is probably due to the different culture condition used (45).

LYN is a positive regulator of PTPs (46, 47), which could be responsible for the decreased tyrosine phosphorylation of several substrates, as shown in Fig. 4A to E. One of the phosphatases involved in the regulation of mast cell degranulation and calcium responses is SHIP1. LYN kinase phosphorylates SHIP1 and thus enhances its enzymatic activity and downregulates degranulation (47, 48). In further experiments, we therefore examined tyrosine phosphorylation of SHIP1 in BMMCs from PAG-WT and PAG-KO mice. In nonactivated WT cells, SHIP1 showed baseline phosphorylation which was enhanced after FcεRI triggering (Fig. 5G and H). Compared to PAG-WT cells, nonactivated PAG-KO cells exhibited significantly higher levels of SHIP1 tyrosine phosphorylation. After activation with antigen, the difference between PAG-WT and PAG-KO cells became insignificant.

Different regulatory roles of PAG in SCF signaling. An important surface receptor of mast cells is KIT, which binds SCF and thereby triggers mast cell activation and enhances activation induced by FcεRI (49). However, no data on the involvement of PAG in SCF-induced activation are available. To determine a possible role of PAG in KIT-mediated activation, PAG-WT and PAG-KO BMMCs were activated with different concentrations of SCF and degranulation was examined. PAG-WT cells released increasing amounts of β-glucuronidase when activated with 25 to 200 ng/ml SCF. The extent of SCF-induced degranulation was higher than that described in previous studies (50, 51) and was apparently related to the growth of bone marrow cells in the presence of both IL-3 and SCF. When BMMCs were derived from cultures containing IL-3 alone, their SCF-induced degranulation was low (45). PAG-KO cells released significantly more β-glucuronidase than PAG-WT cells at all concentrations of SCF tested (Fig. 6A). This effect was associated with higher levels of KIT tyrosine phosphorylation in PAG-KO cells (Fig. 6B and C). However, an opposite effect of PAG on FcεRI- and KIT-mediated signaling events was absent when tyrosine phosphorylation of PLCγ1 was examined. Stimulation of PAG-WT cells with antigen as well as with SCF resulted in tyrosine phosphorylation of PLCγ1, even though it was slower in SCF-activated cells. Similar findings have been previously described (50) and indicate that FcεRI-activated PTKs are more potent for the phosphorylation of PLCγ1 than that of KIT. In PAG-KO cells, the extent of PLCγ1 tyrosine phosphorylation was significantly inhibited in both antigen- and SCF-triggered cells (Fig. 6D and E). A similar effect was observed when PLCγ2 was examined (data not shown). No significant effect of PAG was observed when the tyrosine phosphorylation of several other signaling molecules (SYK, LAT, FAK, paxillin) was examined in PAG-WT and PAG-KO cells. Furthermore, no effect of PAG on the calcium response was observed in SCF-activated BMMCs (not shown).

An important aspect of mast cell physiology is chemotaxis directed by various ligands (52). Here we compared chemotaxis toward antigen or SCF in cells differing in PAG expression. In transwell migration assays, PAG-WT BMMCs exhibited faster migration toward the antigen than PAG-KO cells. The difference was almost 2-fold and was significant (Fig. 6F). When SCF was used as a chemoattractant, both cell types migrated faster and no significant difference between them was evident. To exclude possible compensatory developmental alterations in PAG-KO cells, we also compared the chemotaxis of BMMCs with PAG-KD and their corresponding controls (pLKO cells). We found significantly lower levels of migration of PAG-KD cells than of pLKO cells after exposure to antigen. Again, no significant difference between the two cell types was observed when SCF was used as a chemoattractant (Fig. 6G).

Positive regulatory role of PAG in cytokine and chemokine production. Previous studies showed that activation of mast cells resulted in the rapid tyrosine phosphorylation of several transcription factors. We selected STAT5, which has been extensively studied in FcεRI- or KIT-activated cells (53, 54), as the transcription factor. To elucidate the role of PAG in this process, we examined tyrosine phosphorylation of STAT5 in nonactivated and antigen- or SCF-activated PAG-WT and PAG-KO cells (Fig. 7A and B). Antigen-induced tyrosine phosphorylation of STAT5 was positively regulated by PAG. A significantly lower level of phosphorylation of STAT5 in PAG-KO cells was observable even without activation, but activation intensified the difference. Phosphorylation of STAT5 was also observed in cells stimulated with SCF

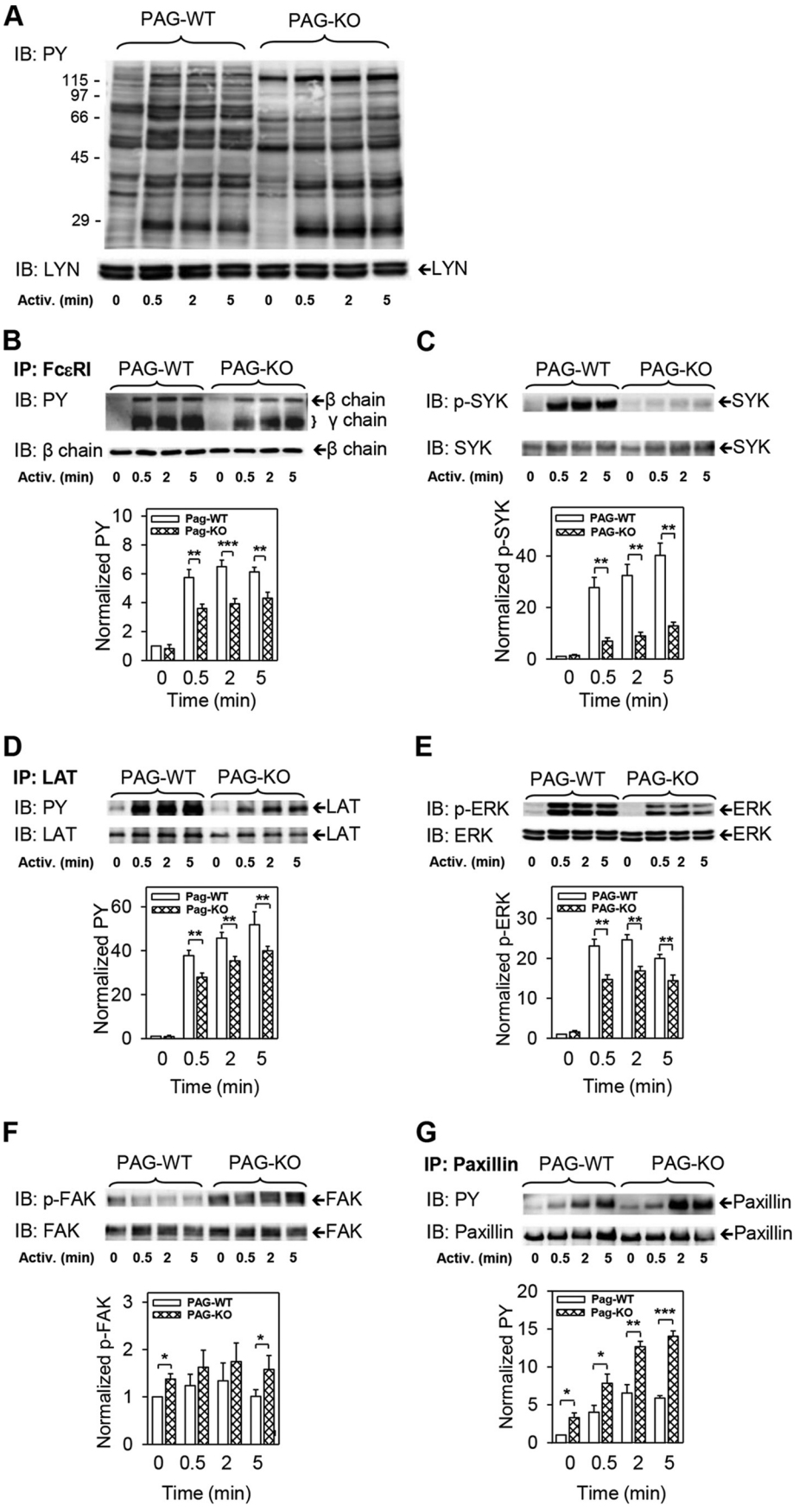
A
PAG-WT
PAG-KO
IB: PY
115 -
97 -
66 -
45 -
29 -
IB: LYN
←LYN
Activ. (min) 0 0.5 2 5 0 0.5 2 5
B
IP: FcεRI
PAG-WT
PAG-KO
IB: PY
←β chain
γ chain
IB: β chain
←β chain
Activ. (min) 0 0.5 2 5 0 0.5 2 5
Pag-WT
Pag-KO
Normalized PY
Time (min)
C
PAG-WT
PAG-KO
IB: p-SYK
←SYK
IB: SYK
←SYK
Activ. (min) 0 0.5 2 5 0 0.5 2 5
PAG-WT
PAG-KO
Normalized p-SYK
Time (min)
D
IP: LAT
PAG-WT
PAG-KO
IB: PY
←LAT
IB: LAT
←LAT
Activ. (min) 0 0.5 2 5 0 0.5 2 5
Pag-WT
Pag-KO
Normalized PY
Time (min)
E
PAG-WT
PAG-KO
IB: p-ERK
←ERK
IB: ERK
←ERK
Activ. (min) 0 0.5 2 5 0 0.5 2 5
PAG-WT
PAG-KO
Normalized p-ERK
Time (min)
F
PAG-WT
PAG-KO
IB: p-FAK
←FAK
IB: FAK
←FAK
Activ. (min) 0 0.5 2 5 0 0.5 2 5
PAG-WT
PAG-KO
Normalized p-FAK
Time (min)
G
IP: Paxillin
PAG-WT
PAG-KO
IB: PY
←Paxillin
IB: Paxillin
←Paxillin
Activ. (min) 0 0.5 2 5 0 0.5 2 5
Pag-WT
Pag-KO
Normalized PY
Time (min)

(Fig. 7A and B). However, no significant difference between PAG-WT and PAG-KO cells was observed.

The decreased phosphorylation of STAT5 in antigen-stimulated PAG-KO cells suggested the reduced production of cytokines and chemokines in such cells (55). Detailed analysis at the protein and mRNA levels showed that, indeed, the levels of three selected cytokines, TNF-α, IL-6, and IL-13, were significantly reduced in antigen-stimulated PAG-KO cells compared with their levels in PAG-WT cells at both the protein and mRNA levels (Fig. 7C). Antigen-activated PAG-KO BMMCs also exhibited significant inhibition of transcription of two chemokines, CCL3 and CCL4 (Fig. 7D).

Phenotype rescue of PAG-KO cells. Next, we attempted to confirm the role of PAG as a positive regulator of cytokine production. We prepared a PAG-myc construct in the pCDH vector and transfected it into PAG-KO BMMCs. Control cells were transfected with the empty pCDH vector, and puromycin-resistant cells were further analyzed. Staining for myc after cell permeabilization and confocal microscopy showed the association of the PAG-myc with the plasma membrane (Fig. 8A). No signal was observed in cells transduced with empty pCDH (Fig. 8B). Furthermore, immunoblotting analysis with Myc tag-specific antibody confirmed the expression of PAG-myc in cells transduced with the pCDH-PAG-myc vector but not the pCDH empty vector (Fig. 8C). These data suggest that PAG-myc was expressed as expected. Next, we examined the production of TNF-α in antigen-activated PAG-WT and PAG-KO cells transfected with empty pCDH and PAG-KO cells transfected with pCDH-PAG-myc. For this analysis we selected flow cytometry, which allowed us to evaluate TNF-α-positive cells, after gating out the cellular debris detected in forward and side scatter plots. This eliminated the problem associated with the presence of different proportions of living cells and debris in various transduction experiments. Data presented in Fig. 8D indicate that the level of production of TNF-α in cells transfected with the empty pCDH vector was significantly lower in PAG-KO cells than in PAG-WT cells. PAG-KO cells transfected with pCDH-PAG-myc produced significantly more TNF-α than pCDH transfectants. These data confirm the phenotype rescue in PAG-KO cells.

Impaired passive systemic anaphylaxis in PAG-KO mice. Finally, we examined degranulation in antigen-activated mast cells under *in vivo* conditions. We induced passive systemic anaphylaxis in PAG-KO and PAG-WT mice by sensitizing them with TNP-specific IgE MAb and subsequent challenge with antigen. In control mice, the decrease in body temperature was observable within the first 60 min and was followed by slow recovery for more than 180 min after antigen injection (Fig. 9A). In PAG-KO mice, the decrease in body temperature was less pronounced and recovery was faster, being complete 150 min after antigen administration. The difference in body temperature between PAG-WT and PAG-KO mice was significant in the interval ranging from 45 to 170 min after antigen administration. The observed decrease in systemic anaphylaxis was not likely attributable to decreased numbers of mast cells in PAG-KO mice, as inferred from comparable mast cell (KIT and FcεRI positive) counts in the peritoneal lavage fluid of PAG-WT and PAG-KO cells (Fig. 9B). Furthermore, we found no significant difference in serum IgE levels between PAG-WT and PAG-KO mice (Fig. 9C). This finding indicates that the production of IgE is not affected by the absence of PAG and that the decreased anaphylactic response in PAG-KO mice is not caused by enhanced production of IgE, which might preclude sensitization with antigen-specific IgE.

DISCUSSION

In this study, we used BMMCs derived from PAG-KO and PAG-WT mice to understand the role of PAG in FcεRI and SCF signaling. To minimize the possible effect of compensatory developmental alterations in PAG-KO cells, we also used BMMCs with PAG-KD and corresponding controls. Several lines of evidence indicate that PAG has positive as well as negative regulatory roles in FcεRI- or KIT-mediated signaling, depending on the receptor triggered and the signaling pathway involved.

First, when stimulated with antigen, mast cells derived from PAG-KO mice exhibited decreased degranulation. In view of previous results obtained with other immunoreceptors (17, 18, 26), this was an unexpected finding because phosphorylated PAG was regarded as a plasma membrane anchor of CSK, a negative regulator of SFKs. Furthermore, overexpression of PAG reportedly resulted in decreased degranulation in RBL-2H3 cells (21). The positive regulatory role of PAG in FcεRI-mediated signaling described here was not the consequence of developmental changes caused by the absence of PAG, since a similar phenotype was also observed in PAG-KD BMMCs where PAG expression was downregulated by RNA interference, nor was the decreased degranulation caused by the reduced production of β-glucuronidase or the reduced expression of FcεRI in PAG-KO and PAG-KD cells. Interestingly, a defect in degranulation was also observed in PAG-deficient cells activated by thapsigargin, a noncompetitive inhibitor of ER Ca^{2+} ATPase.

Second, antigen-activated PAG-KO cells exhibited decreased tyrosine phosphorylation of FcεRI β and γ subunits. This change implies that the reduced degranulation in PAG-deficient cells is caused at least in part by inhibition of the earliest stages of mast cell signaling, starting from reduced phosphorylation of the FcεRI β and γ subunits, followed by impaired membrane anchoring, phosphorylation, and activation of SYK. The exact molecular mechanism of the impaired phosphorylation of FcεRI in PAG-

FIG 4 Antigen-induced tyrosine phosphorylation of signal transduction proteins is dependent on PAG. (A to G) IgE-sensitized PAG-WT and PAG-KO cells were activated (Activ.) for the indicated time intervals with antigen (250 ng/ml). The cells were lysed, and total cellular lysates were analyzed by immunoblotting with the tyrosine-specific MAb PY-20–HRP conjugate (PY). Alternatively, FcεRI (B), LAT (D), and paxillin (G) were immunoprecipitated (IP) from the lysates and examined by immunoblotting with tyrosine-specific MAb as in the experiment whose results are shown in panel A. For SYK (C), ERK (E), and FAK (F), size-fractionated proteins in cell lysates were directly analyzed by immunoblotting with the corresponding phosphoprotein-specific antibodies. For loading controls, the membranes were analyzed by immunoblotting for LYN kinase (A), the FcεRI β chain (B), SYK (C), LAT (D), ERK (E), FAK (F), and paxillin (G). Panel A and the tops of panels B to G show representative immunoblots from at least three experiments. The bottoms of panels B to G show the results of densitometry analysis of the corresponding immunoblots in which signals from tyrosine-phosphorylated proteins in activated cells were normalized to the signals in nonactivated cells and loading control proteins. Means ± SEs were calculated from a minimum of four independent experiments. The statistical significance of the differences between PAG-WT and PAG-KO cells is also shown: *, $P < 0.05$; **, $P < 0.01$; ***, $P < 0.001$. p-SYK, p-ERK, and p-FAK, phosphorylated SYK, ERK, and FAK, respectively.

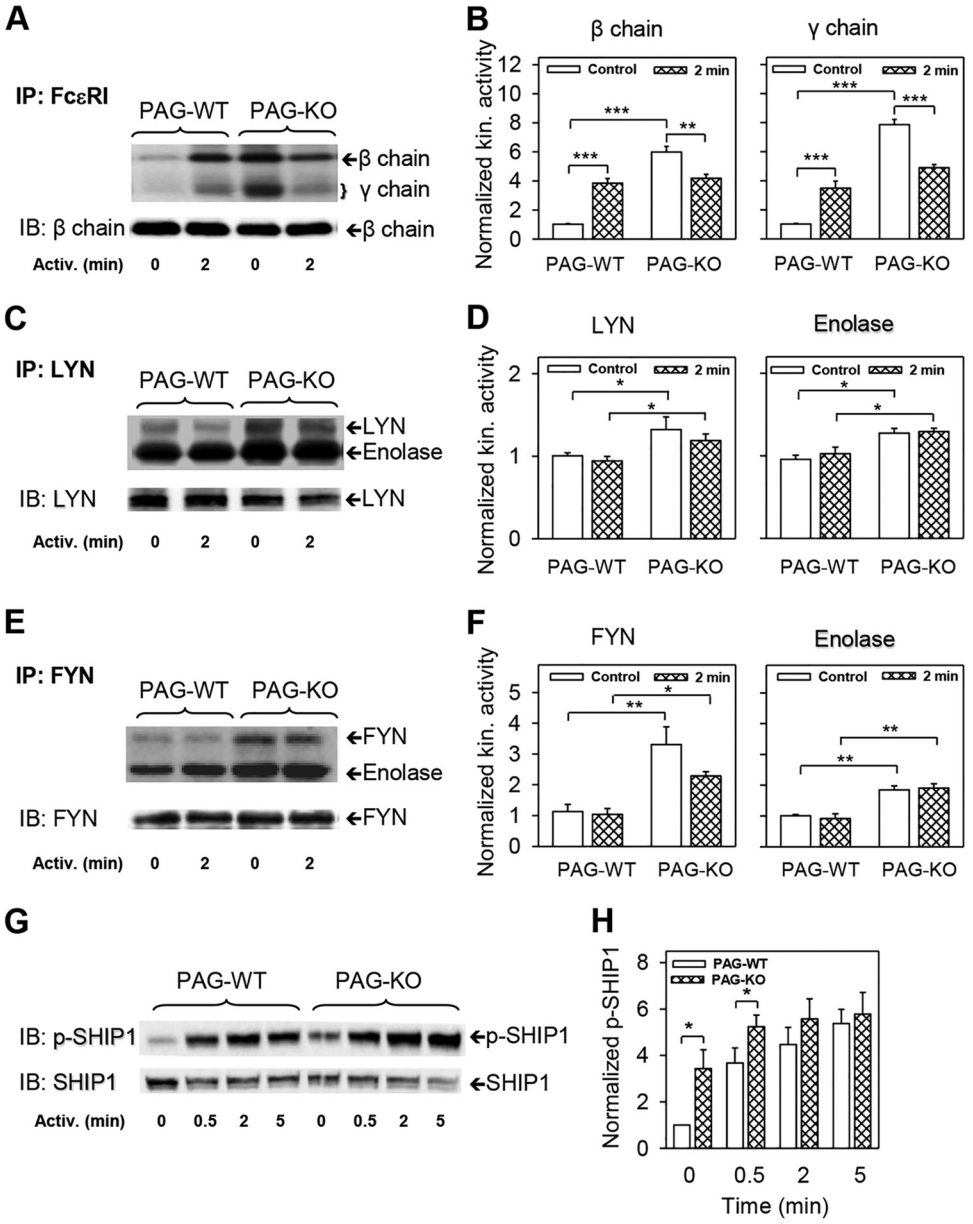

FIG 5 PAG-dependent regulation of LYN and FYN kinase (kin.) activities and SHIP1 tyrosine phosphorylation. (A) IgE-sensitized PAG-WT and PAG-KO BMMCs were activated or not for 2 min with antigen (250 ng/ml) and then solubilized with lysis buffer containing 1% Brij 96. FcεRI-IgE complexes were immunoprecipitated and incubated in a kinase buffer containing [γ-^{32}P]ATP. After the kinase assay, ^{32}P-labeled proteins were size fractionated, transferred to nitrocellulose membranes, and examined by autoradiography. The relative amounts of the FcεRI β chain were determined by immunoblotting. The positions of FcεRI β and γ chains are indicated. (B) Autoradiograms obtained as described in the legend to panel A were quantified, and the signals corresponding to the FcεRI β and γ chains were normalized to the signals in nonactivated PAG-WT cells and the amount of FcεRI β chain immunoprecipitated. (C to F) The cells were activated and solubilized as described in the legend to panel A. LYN (C and D) and FYN (E and F) were immunoprecipitated and incubated in kinase buffer supplemented with [γ-^{32}P]ATP and acid-denatured enolase, used as an exogenous substrate. Kinase assays and further analyses were performed as described in the legend to panel A. Autoradiograms were quantified, and the signals corresponding to LYN, FYN, and enolase were normalized to the signals in nonactivated PAG-WT cells and the amount of immunoprecipitated LYN (D) or FYN (F). (G and H) IgE-sensitized PAG-WT and PAG-KO BMMCs were activated for the indicated time intervals with antigen as described in the legend to panel A. The cells were lysed and analyzed by immunoblotting with phosphorylated-SHIP1 (p-SHIP1)-specific antibody. The amount of SHIP1 was used as a loading control. (H) Densitometry analysis of the immunoblots in which the signal for phospho-SHIP1 was normalized to the signal in nonactivated PAG-WT cells and the amount of SHIP1. The results of representative experiments are shown in panels A, C, E, and G. The means ± SEs in panels B, D, F, and H were calculated from three to five independent experiments. The statistical significance of intergroup differences is indicated: *, $P < 0.05$; **, $P < 0.01$; ***, $P < 0.001$.

deficient cells is unknown and is likely connected to local changes in the activity and/or the topography of SFKs and PTPs within the FcεRI signalosome. Our finding that FcεRI immunocomplexes isolated from nonionic detergent-solubilized nonactivated PAG-KO cells show kinase activity higher than those isolated from PAG-WT cells would be compatible with this hypothesis, provided that PTKs are more stably associated with isolated FcεRI immunocomplexes than PTPs. Furthermore, we found that ty-

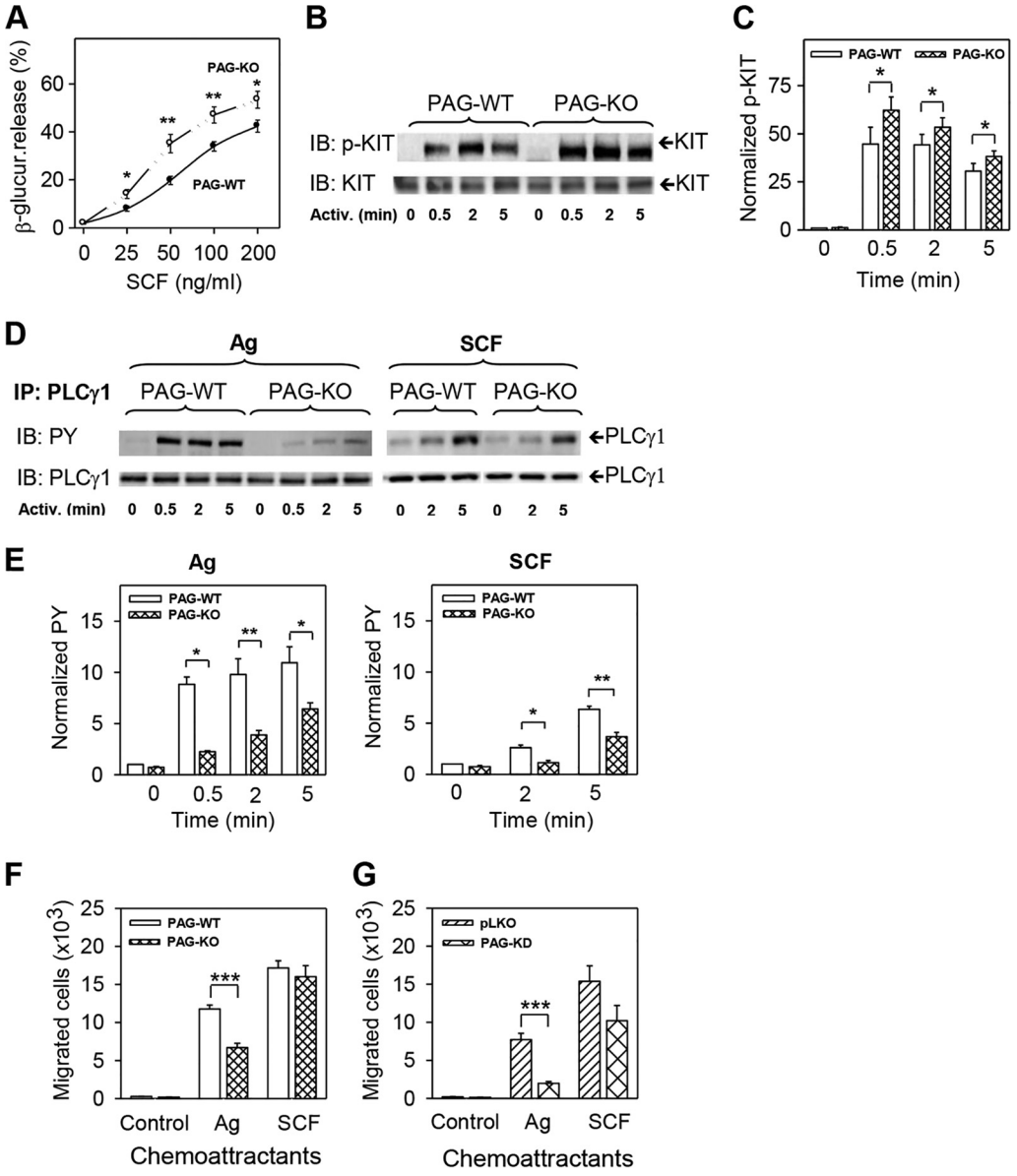

FIG 6 Different regulatory roles of PAG in KIT and FcεRI signaling. (A) PAG-WT and PAG-KO BMMCs were stimulated for 30 min with various concentrations of SCF, and the amount of β-glucuronidase released into the supernatant was determined. (B) PAG-WT and PAG-KO cells were exposed to SCF (50 ng/ml) for different time intervals and lysed, and tyrosine phosphorylation of KIT was analyzed by immunoblotting with phosphorylated-KIT (p-KIT)-specific antibody. Immunoblotting with KIT-specific antibody served as a loading control. The results of one representative experiment out of three performed are shown. (C) The immunoblots obtained as described in the legend to panel B were analyzed by densitometry, and the amounts of tyrosine-phosphorylated KIT were normalized to the amounts of tyrosine-phosphorylated KIT in nonactivated PAG-WT cells and loading controls. (D and E) PAG-WT and PAG-KO BMMCs were activated for different time intervals with antigen (250 ng/ml) or SCF (50 ng/ml) and lysed, and PLCγ1 was immunoprecipitated. The immunoprecipitates were analyzed by immunoblotting with tyrosine-specific MAb PY-20–HRP conjugate (PY) (D). As loading controls, the membranes were also analyzed by immunoblotting for PLCγ1. Representative immunoblots out of three performed are shown. The immunoblots obtained were analyzed by densitometry, and the relative amounts of tyrosine-phosphorylated proteins were normalized to the amounts of the proteins immunoprecipitated and to the amounts of tyrosine-phosphorylated proteins in nonactivated PAG-WT cells (E). (F) IgE-sensitized PAG-WT or PAG-KO BMMCs were analyzed in a chemotactic assay with chemotaxis medium alone (Control) or with chemotaxis medium supplemented with antigen (250 ng/ml) or SCF (100 ng/ml) in the lower wells. The numbers of cells migrating into the lower wells were determined after 8 h. (G) The experiments were performed as described in the legend to panel F, except that cells with PAG-KD and the corresponding controls (pLKO) were used. Means ± SEs were calculated from a minimum of nine independent experiments performed in triplicate (A), three independent experiments (C, E, and G), or six independent experiments (F). The statistical significance of differences between PAG-WT/PAG-KO cells (A, C, E, and F) and pLKO/PAG-KD cells (G) is shown: *, $P < 0.05$; **, $P < 0.01$; ***, $P < 0.001$.

rosine phosphorylation of SHIP1, a negative regulator of mast cell activation (48, 56), is increased in nonactivated PAG-KO cells. This could be caused by the enhanced enzymatic activity of LYN, which phosphorylates and activates SHIP1 (47), and in this manner could contribute to decreased calcium and degranulation responses (48, 56).

In contrast to FcεRI and several other signaling proteins involved in the calcium response (SYK, LAT, and PLCγ), FAK and at

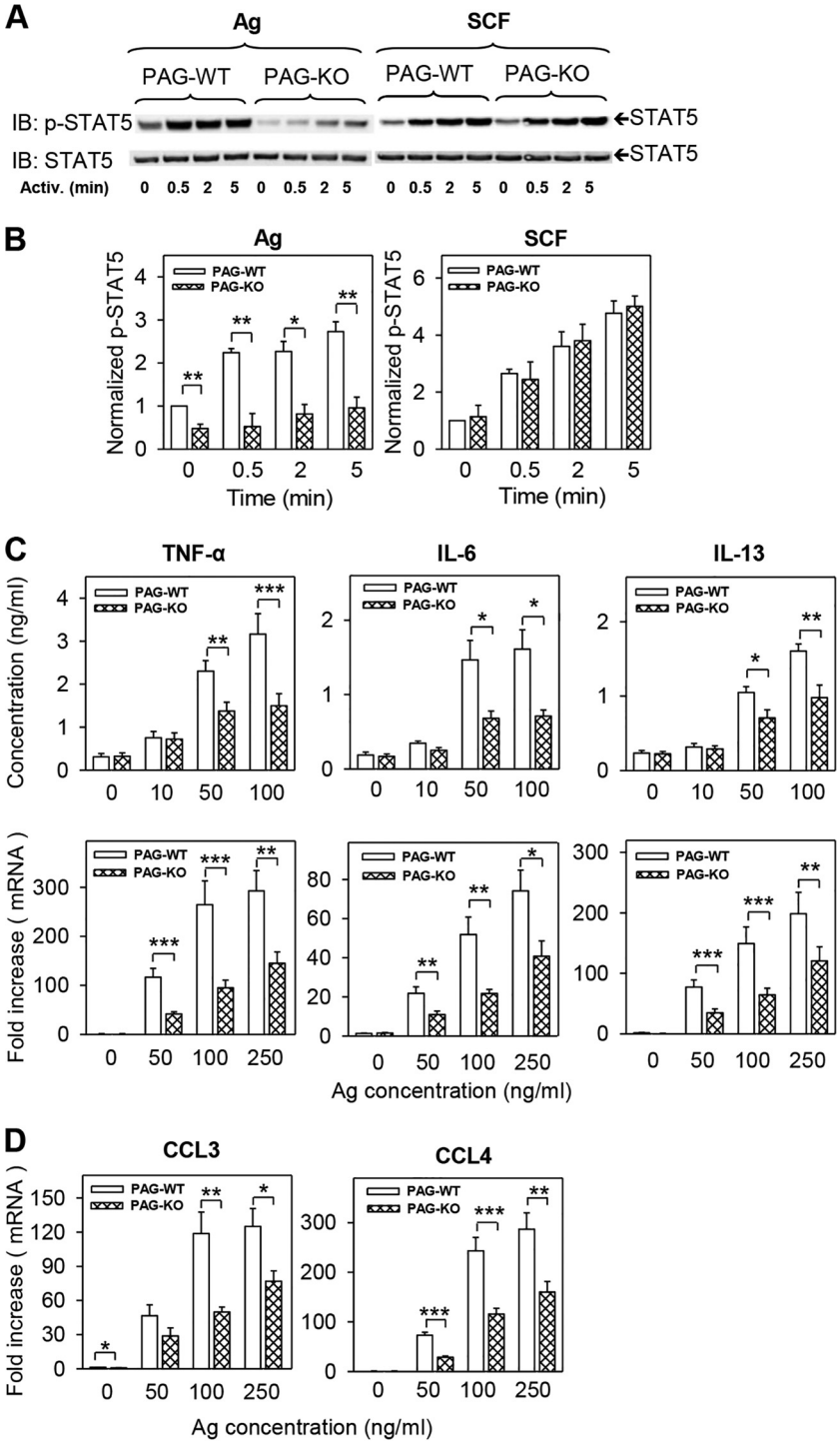

FIG 7 Decreased tyrosine phosphorylation of STAT5 and production of cytokines and chemokines in antigen-activated PAG-KO BMMCs. (A) Cells were activated for different time intervals with antigen (250 ng/ml) or SCF (50 ng/ml), lysed, and analyzed for STAT5 tyrosine 694 phosphorylation by immunoblotting. As loading controls, the membranes were also immunoblotted with STAT5-specific antibody. Representative immunoblots are shown. (B) The immunoblots were analyzed by densitometry, and the relative amount of tyrosine-phosphorylated STAT5 (p-STAT5) was normalized to its amount in nonactivated cells and the corresponding loading control. (C, D) The levels of production of cytokines (TNF-α, IL-6, and IL-13) at the protein level (C, top) and mRNA level (C, bottom) and chemokines (CCL3 and CCL4) (D) were evaluated at the mRNA level in PAG-WT and PAG-KO BMMCs activated with various concentrations of antigen for 1 h (mRNA) or 6 h (protein). Specific proteins and mRNAs were quantified by immuno-PCR and qPCR, respectively. Means ± SEs were calculated from 4 to 12 independent experiments. The statistical significance of differences between PAG-WT and PAG-KO cells is shown: *, $P < 0.05$; **, $P < 0.01$; ***, $P < 0.001$.

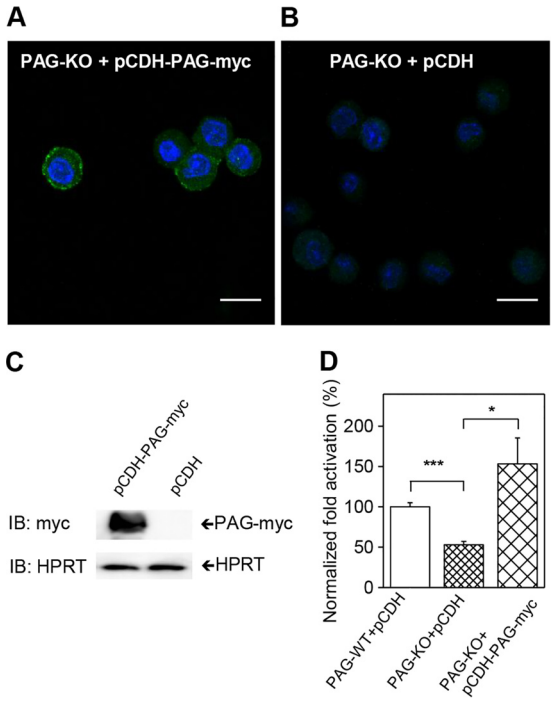

FIG 8 Phenotype rescue of PAG-KO BMMCs. (A, B) PAG-KO BMMCs were transfected with the pCDH-PAG-myc vector (A) or the control empty vector (pCDH) (B). Puromycin-resistant transfectants were isolated and attached to fibronectin-coated slides. Then, the cells were fixed, permeabilized, and labeled for PAG-myc with an anti-Myc tag/anti-IgG–Alexa Fluor 488 conjugate (green) and Hoechst 33258 (blue). Bars, 10 μm. (C) Puromycin-resistant pCDH-PAG-myc- or empty pCDH vector-transfected cells were solubilized, and the presence of PAG-myc was determined by immunoblotting with anti-Myc tag antibody. As loading controls, the membranes were developed for HPRT. (D) PAG-WT or PAG-KO BMMCs stably transfected with the pCDH vector (PAG-WT+pCDH and PAG-KO+pCDH, respectively) or PAG-KO BMMCs transfected with pCDH-PAG-myc (PAG-KO+pCDH-PAG-myc) were sensitized overnight with IgE and then activated with antigen (100 ng/ml). After 90 min the cells were fixed and stained with TNF-α specific rabbit antibody, followed by anti-rabbit IgG–Alexa Fluor 488 conjugate. The cells were analyzed by flow cytometry, and the ratios of the mean fluorescence intensity between activated and nonactivated cells were normalized to those for the pCDH-transfected PAG-WT controls. Data show means ± SEs calculated from three independent experiments. The statistical significance of the differences is indicated: *, $P < 0.05$; ***, $P < 0.001$.

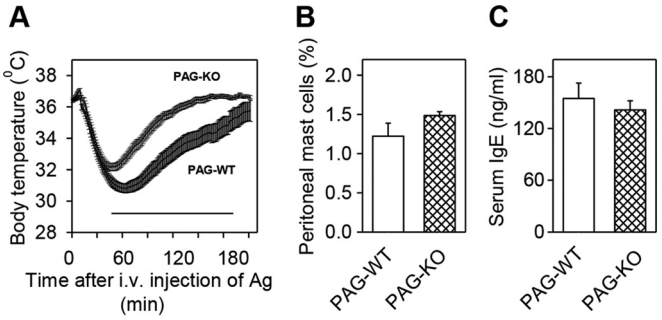

FIG 9 Decreased passive systemic anaphylaxis in PAG-KO mice. (A) PAG-WT ($n = 17$) and PAG-KO mice ($n = 16$) were passively sensitized with TNP-specific IgE (3 μg/mouse) and 24 h later were challenged with antigen (500 μg per mouse) to induce systemic anaphylaxis. Body temperature responses at various time intervals after antigen administration were recorded. Means ± SEs are shown. Statistically significant differences ($P < 0.05$) between PAG-WT and PAG-KO mice are indicated by the black line below the curves. i.v., intravenous. (B) Percentage of mast cells (KIT and FcεRI positive) in peritoneal lavage fluid of PAG-WT and PAG-KO mice. (C) Serum IgE levels in PAG-WT and PAG-KO mice. Data are means ± SEs calculated for three (B) or four (C) animals in each group.

least one of its substrates, the multidomain scaffolding adaptor protein paxillin, showed enhanced tyrosine phosphorylation in PAG-KO cells. The molecular mechanism of enhanced phosphorylation of FAK and paxillin in PAG-KO cells remains to be determined but apparently reflects changes in the activity of SFKs and PTPs which use FAK and paxillin as a substrate (57, 58).

Third, PAG-deficient BMMCs showed reduced calcium uptake after activation with antigen. This could be attributed to the reduced tyrosine phosphorylation and activity of PLCγ, which cleaves the plasma membrane-bound phosphatidylinositol 4,5-bisphosphate into diacylglycerol and inositol 1,4,5-trisphosphate; the latter binds to its receptors and regulates the release of calcium from intracellular organelles. Increases in cytoplasmic calcium lead to the influx of extracellular calcium into the cytoplasm through SOC channels. Reduced calcium uptake in PAG-KO cells was observed not only after exposure to antigen but also after activation with thapsigargin. This could be related to previous findings documenting that PLCγ is involved in thapsigargin-induced Ca^{2+} entry (59–61) and reduced phosphorylation of PLCγ in PAG-deficient cells. Furthermore, it has been shown that STIM1, which is indispensable for opening SOC channels in mast cells (62, 63), needs for its function expression and phosphorylation of SYK and LYN kinases (64). Enhanced tyrosine phosphorylation of SHIP1 and, presumably, its increased enzymatic activity (45, 46) could also contribute to decreased calcium mobilization in activated PAG-KO cells.

Fourth, PAG-KO cells exhibited higher degranulation when activated by SCF. SCF binds to KIT, a type III plasma membrane receptor tyrosine kinase. After SCF binding, the receptor forms a dimer that stimulates its intrinsic tyrosine kinase activity, creating phosphotyrosine binding sites for FYN (65) and LYN (66) kinases and many other signaling molecules, including SHIP1 and PLCγ (67). These molecules are apparently integrated into signaling circuits regulated by PAG.

Fifth, it has previously been shown that activation through FcεRI as well as KIT rapidly stimulates STAT5 tyrosine phosphorylation and that STAT5 deficiency greatly reduces early and late mast cell responses (68). PAG-KO cells exhibited lower tyrosine phosphorylation of STAT5 when activated via FcεRI but not when activated via KIT. This difference could be explained by the different kinases involved in STAT5 phosphorylation. In SCF-activated cells, KIT activates STAT5 partly through the tyrosine kinase JAK2 (69). In contrast, JAK2 is dispensable in IgE-activated cells, which use FYN for STAT5 phosphorylation (53). Phosphorylated STAT5 serves as a transcription factor for a number of inflammatory genes (55). The reduced transcription of genes for cytokines (TNF-α, IL-6, and IL-13) and chemokines (CCL3 and CCL4) and the reduced production of TNF-α, IL-6, and IL-13 in antigen-activated PAG-KO cells could be a direct consequence of impaired STAT5 tyrosine phosphorylation.

Sixth, IgE-sensitized PAG-KO cells exhibited decreased chemotaxis toward antigen. Mast cell chemotaxis is a complex process dependent on numerous signaling molecules and cell signaling pathways (52). The observed inhibition of tyrosine phosphorylation of the FcεRI β and γ subunits, SYK, and LAT in an-

tigen-activated PAG-deficient cells could partly explain the reduced antigen-induced chemotaxis (70). In contrast, PAG-KO BMMCs showed no inhibition of KIT and LAT tyrosine phosphorylation after SCF triggering, and this could be related to a normal chemotaxis response toward SCF in these cells. These findings indicate that either PAG is not involved in the regulation of KIT-mediated chemotaxis or the positive regulatory roles of PAG are compensated for by activation of other molecules, such as PTPs, which also bind to KIT (71, 72).

Seventh, experiments *in vivo* showed that PAG is a positive regulator of passive systemic anaphylaxis, manifested by a decreased body temperature after administration of antigen into IgE-sensitized mice. It is widely accepted that the anaphylactic reaction is initiated by inflammatory mediators released from mast cells (73, 74). Experiments with mice deficient in histidine decarboxylase and therefore lacking histamine suggested that the histamine released from mast cells controls body temperature (39). Our finding of impaired degranulation in PAG-KO cells could thus be directly related to the impaired anaphylactic response. A positive regulatory role of PAG in passive systemic anaphylaxis is the first well-defined *in vivo* trait that is regulated by PAG.

Although previous data from studies using other cell types have implicated the phosphorylation of PAG and PAG-CSK interactions as an important regulatory step in immunoreceptor signaling (11, 12), no dramatic changes in tyrosine phosphorylation of PAG were observed in the course of FcεRI-mediated activation of BMMCs (19; our unpublished data). Furthermore, only a small fraction of CSK colocalized with PAG in lipid raft fractions in PAG-WT BMMCs. In PAG-KO cells, CSK was not detected in lipid raft fractions, suggesting that in mast cells PAG could be a major anchor of CSK in lipid rafts. These data corroborate the results of a previous study documenting that PAG in lipid rafts from mouse thymocytes is a major anchor of CSK (18). On the other hand, they stand in contrast to the findings of another study (17) showing that the amount of lipid raft-associated CSK in thymus cells is not affected by the absence of PAG. However, we would like to point out that different detergents and cell/detergent ratios were used in these various studies and that the association of proteins with lipid rafts is sensitive to these parameters (75, 76).

In summary, the data reported in this study provide compelling evidence that PAG functions as both a positive and a negative regulator of mast cell signaling, depending on the signaling pathway involved. It seems that through interaction with CSK, PAG serves as a negative regulator of SFKs, which are involved in both positive and negative regulatory loops in mast cell activation. Furthermore, we show for the first time that PAG-deficient mice exhibit a distinct phenotype in terms of a passive systemic anaphylaxis response.

ACKNOWLEDGMENTS

We thank H. Mrazova, L. Kocanda, and R. Budovicova for technical assistance.

This work was supported by projects 301/09/1826, P302/10/1759, P302-14-09807S, P302/12/G101, P305-14-00703S, and 204/09/H084 from the Czech Science Foundation, by Action BM1007 from European Cooperation in Science and Technology, by project LD12073 COST-CZ-MAST from the Ministry of Education, Youth, and Sports of the Czech Republic, and by the Institute of Molecular Genetics of the Academy of Sciences of the Czech Republic (RVO 68378050). L.P., M.B., and I.P. were supported in part by the Faculty of Science, Charles University, Prague, Czech Republic.

We have no conflicting financial interests.

REFERENCES

1. **Galli SJ, Borregaard N, Wynn TA.** 2011. Phenotypic and functional plasticity of cells of innate immunity: macrophages, mast cells and neutrophils. Nat. Immunol. **12:**1035–1044. http://dx.doi.org/10.1038/ni.2109.
2. **Eiseman E, Bolen JB.** 1992. Engagement of the high-affinity IgE receptor activates *src* protein-related tyrosine kinases. Nature **355:**78–80. http://dx.doi.org/10.1038/355078a0.
3. **Yamashita T, Mao S-Y, Metzger H.** 1994. Aggregation of the high-affinity IgE receptor and enhanced activity of p53/p56^{lyn} protein-tyrosine kinase. Proc. Natl. Acad. Sci. U. S. A. **91:**11251–11255. http://dx.doi.org/10.1073/pnas.91.23.11251.
4. **Pribluda VS, Pribluda C, Metzger H.** 1994. Transphosphorylation as the mechanism by which the high-affinity receptor for IgE is phosphorylated upon aggregation. Proc. Natl. Acad. Sci. U. S. A. **91:**11246–11250. http://dx.doi.org/10.1073/pnas.91.23.11246.
5. **Field KA, Holowka D, Baird B.** 1995. FcεRI-mediated recruitment of p53/56^{lyn} to detergent-resistant membrane domains accompanies cellular signaling. Proc. Natl. Acad. Sci. U. S. A. **92:**9201–9205. http://dx.doi.org/10.1073/pnas.92.20.9201.
6. **Heneberg P, Dráberová L, Bambousková M, Pompach P, Dráber P.** 2010. Down-regulation of protein tyrosine phosphatases activates an immune receptor in the absence of its translocation into lipid rafts. J. Biol. Chem. **285:**12787–12802. http://dx.doi.org/10.1074/jbc.M109.052555.
7. **Tolar P, Dráberová L, Tolarová H, Dráber P.** 2004. Positive and negative regulation of Fcε receptor I-mediated signaling events by Lyn kinase C-terminal tyrosine phosphorylation. Eur. J. Immunol. **34:**1136–1145. http://dx.doi.org/10.1002/eji.200324505.
8. **Bergman M, Mustelin T, Oetken C, Partanen J, Flint NA, Amrein KA, Autero M, Burn P, Alitalo K.** 1992. The human p50 csk tyrosine kinase phosphorylates p56 lck at tyr-505 and down regulates its catalytic activity. EMBO J. **11:**2919–2924.
9. **Plas DR, Thomas ML.** 1998. Negative regulation of antigen receptor signaling in lymphocytes. J. Mol. Med. (Berl.) **76:**589–595. http://dx.doi.org/10.1007/s001090050254.
10. **Nada S, Okada M, MacAuley A, Cooper JA, Nakagawa H.** 1991. Cloning of a complementary DNA for a protein-tyrosine kinase that specifically phosphorylates a negative regulatory site for p60$^{c\text{-}src}$. Nature **351:**69–72. http://dx.doi.org/10.1038/351069a0.
11. **Brdička T, Pavlistová D, Leo A, Bruyns E, Kořínek V, Angelisová P, Scherer J, Shevchenko A, Hilgert I, Černý J, Drbal K, Kuramitsu Y, Kornacker B, Hořejší V, Schraven B.** 2000. Phosphoprotein associated with glycosphingolipid-enriched microdomains (PAG), a novel ubiquitously expressed transmembrane adaptor protein, binds the protein tyrosine kinase csk and is involved in regulation of T cell activation. J. Exp. Med. **191:**1591–1604. http://dx.doi.org/10.1084/jem.191.9.1591.
12. **Kawabuchi M, Satomi Y, Takao T, Shimonishi Y, Nada S, Nagai K, Tarakhovsky A, Okada M.** 2000. Transmembrane phosphoprotein Cbp regulates the activities of Src-family tyrosine kinases. Nature **404:**999–1003. http://dx.doi.org/10.1038/35010121.
13. **Brdičková N, Brdička T, Anděra L, Špička J, Angelisová P, Milgram SL, Hořejší V.** 2001. Interaction between two adapter proteins, PAG and EBP50: a possible link between membrane rafts and actin cytoskeleton. FEBS Lett. **507:**133–136. http://dx.doi.org/10.1016/S0014-5793(01)02955-6.
14. **Draber P, Halova I, Levi-Schaffer F, Draberova L.** 2012. Transmembrane adaptor proteins in the high-affinity IgE receptor signaling. Front. Immunol. **2:**1–11. http://dx.doi.org/10.3389/fimmu.2011.00095.
15. **Hrdinka M, Horejsi V.** 11 November 2013. PAG—a multipurpose transmembrane adaptor protein. Oncogene http://dx.doi.org/10.1038/onc.2013.485.
16. **Smida M, Cammann C, Gurbiel S, Kerstin N, Lingel H, Lindquist S, Simeoni L, Brunner-Weinzierl MC, Suchanek M, Schraven B, Lindquist JA.** 2013. PAG/Cbp suppression reveals a contribution of CTLA-4 to setting the activation threshold in T cells. Cell Commun. Signal. **11:**28. http://dx.doi.org/10.1186/1478-811X-11-28.
17. **Dobenecker MW, Schmedt C, Okada M, Tarakhovsky A.** 2005. The ubiquitously expressed Csk adaptor protein Cbp is dispensable for embryogenesis and T-cell development and function. Mol. Cell. Biol. **25:**10533–10542. http://dx.doi.org/10.1128/MCB.25.23.10533-10542.2005.

18. **Xu S, Huo J, Tan JE, Lam KP.** 2005. Cbp deficiency alters Csk localization in lipid rafts but does not affect T-cell development. Mol. Cell. Biol. **25:**8486–8495. http://dx.doi.org/10.1128/MCB.25.19.8486-8495.2005.
19. **Odom S, Gomez G, Kovarova M, Furumoto Y, Ryan JJ, Wright HV, Gonzalez-Espinosa C, Hibbs ML, Harder KW, Rivera J.** 2004. Negative regulation of immunoglobulin E-dependent allergic responses by Lyn kinase. J. Exp. Med. **199:**1491–1502. http://dx.doi.org/10.1084/jem.20040382.
20. **Kitaura J, Kawakami Y, Maeda-Yamamoto M, Horejsi V, Kawakami T.** 2007. Dysregulation of Src family kinases in mast cells from epilepsy-resistant ASK versus epilepsy-prone EL mice. J. Immunol. **178:**455–462. http://dx.doi.org/10.4049/jimmunol.178.1.455.
21. **Ohtake H, Ichikawa N, Okada M, Yamashita T.** 2002. Cutting edge: transmembrane phosphoprotein Csk-binding protein/phosphoprotein associated with glycosphingolipid-enriched microdomains as a negative feedback regulator of mast cell signaling through the FcεRI. J. Immunol. **168:**2087–2090. http://dx.doi.org/10.4049/jimmunol.168.5.2087.
22. **Nishizumi H, Horikawa K, Mlinaric-Rascan I, Yamamoto T.** 1998. A double-edged kinase Lyn: a positive and negative regulator for antigen receptor-mediated signals. J. Exp. Med. **187:**1343–1348. http://dx.doi.org/10.1084/jem.187.8.1343.
23. **Kawakami Y, Kitaura J, Satterthwaite AB, Kato RM, Asai K, Hartman SE, Maeda-Yamamoto M, Lowell CA, Rawlings DJ, Witte ON, Kawakami T.** 2000. Redundant and opposing functions of two tyrosine kinases, Btk and Lyn, in mast cell activation. J. Immunol. **165:**1210–1219. http://dx.doi.org/10.4049/jimmunol.165.3.1210.
24. **Parravicini V, Gadina M, Kovarova M, Odom S, Gonzalez-Espinosa C, Furumoto Y, Saitoh S, Samelson LE, O'Shea JJ, Rivera J.** 2002. Fyn kinase initiates complementary signals required for IgE-dependent mast cell degranulation. Nat. Immunol. **3:**741–748. http://dx.doi.org/10.1038/ni817.
25. **Yang Y, Seed B.** 2003. Site-specific gene targeting in mouse embryonic stem cells with intact bacterial artificial chromosomes. Nat. Biotechnol. **21:**447–451. http://dx.doi.org/10.1038/nbt803.
26. **Lindquist S, Karitkina D, Langnaese K, Posevitz-Fejfar A, Schraven B, Xavier R, Seed B, Lindquist JA.** 2011. Phosphoprotein associated with glycosphingolipid-enriched microdomains differentially modulates SRC kinase activity in brain maturation. PLoS One **6:**e23978. http://dx.doi.org/10.1371/journal.pone.0023978.
27. **National Research Council.** 2011. Guide for the care and use of laboratory animals, 8th ed. National Academies Press, Washington, DC.
28. **Tolar P, Tůmová M, Dráber P.** 2001. New monoclonal antibodies recognizing the adaptor protein LAT. Folia Biol. (Praha) **47:**215–217.
29. **Dráberová L, Amoui M, Dráber P.** 1996. Thy-1-mediated activation of rat mast cells: the role of Thy-1 membrane microdomains. Immunology **87:**141–148.
30. **Rivera J, Kinet J-P, Kim J, Pucillo C, Metzger H.** 1988. Studies with a monoclonal antibody to the β subunit of the receptor with high affinity for immunoglobulin E. Mol. Immunol. **25:**647–661. http://dx.doi.org/10.1016/0161-5890(88)90100-9.
31. **Rudolph AK, Burrows PD, Wabl MR.** 1981. Thirteen hybridomas secreting hapten-specific immunoglobulin E from mice with Ig^a or Ig^b heavy chain haplotype. Eur. J. Immunol. **11:**527–529. http://dx.doi.org/10.1002/eji.1830110617.
32. **Kovářová M, Tolar P, Arudchandran R, Dráberová L, Rivera J, Dráber P.** 2001. Structure-function analysis of Lyn kinase association with lipid rafts and initiation of early signaling events after Fcε receptor I aggregation. Mol. Cell. Biol. **21:**8318–8328. http://dx.doi.org/10.1128/MCB.21.24.8318-8328.2001.
33. **Surviladze Z, Dráberová L, Kovářová M, Boubelík M, Dráber P.** 2001. Differential sensitivity to acute cholesterol lowering of activation mediated via the high-affinity IgE receptor and Thy-1 glycoprotein. Eur. J. Immunol. **31:**1–10. http://dx.doi.org/10.1002/1521-4141(200101)31:1<1::AID-IMMU1>3.0.CO;2-W.
34. **Dráberová L.** 1990. Cyclosporin A inhibits rat mast cell activation. Eur. J. Immunol. **20:**1469–1473. http://dx.doi.org/10.1002/eji.1830200710.
35. **Surviladze Z, Dráberová L, Kubínová L, Dráber P.** 1998. Functional heterogeneity of Thy-1 membrane microdomains in rat basophilic leukemia cells. Eur. J. Immunol. **28:**1847–1858. http://dx.doi.org/10.1002/(SICI)1521-4141(199806)28:06<1847::AID-IMMU1847>3.0.CO;2-O.
36. **Amoui M, Dráber P, Dráberová L.** 1997. Src family-selective tyrosine kinase inhibitor, PP1, inhibits both FcεRI- and Thy-1-mediated activation of rat basophilic leukemia cells. Eur. J. Immunol. **27:**1881–1886. http://dx.doi.org/10.1002/eji.1830270810.
37. **Horáková H, Polakovičová I, Shaik GM, Eitler J, Bugajev V, Dráberová L, Dráber P.** 2011. 1,2-Propanediol-trehalose mixture as a potent quantitative real-time PCR enhancer. BMC Biotechnol. **11:**41. http://dx.doi.org/10.1186/1472-6750-11-41.
38. **Potůčková L, Franko F, Bambousková M, Dráber P.** 2011. Rapid and sensitive detection of cytokines using functionalized gold nanoparticle-based immuno-PCR, comparison with immuno-PCR and ELISA. J. Immunol. Methods **371:**38–47. http://dx.doi.org/10.1016/j.jim.2011.06.012.
39. **Makabe-Kobayashi Y, Hori Y, Adachi T, Ishigaki-Suzuki S, Kikuchi Y, Kagaya Y, Shirato K, Nagy A, Ujike A, Takai T, Watanabe T, Ohtsu H.** 2002. The control effect of histamine on body temperature and respiratory function in IgE-dependent systemic anaphylaxis. J. Allergy Clin. Immunol. **110:**298–303. http://dx.doi.org/10.1067/mai.2002.125977.
40. **Thastrup O, Dawson AP, Scharff O, Foder B, Cullen PJ, Drobak BK, Bjerrum PJ, Christensen SB, Hanley MR.** 1989. Thapsigargin, a novel molecular probe for studying intracellular calcium release and storage. Agents Actions **27:**17–23. http://dx.doi.org/10.1007/BF02222186.
41. **Putney JW, Jr.** 2005. Capacitative calcium entry: sensing the calcium stores. J. Cell Biol. **169:**381–382. http://dx.doi.org/10.1083/jcb.200503161.
42. **Volná P, Lebduška P, Dráberová L, Šímová S, Heneberg P, Boubelík M, Bugajev V, Malissen B, Wilson BS, Hořejší V, Malissen M, Dráber P.** 2004. Negative regulation of mast cell signaling and function by the adaptor LAB/NTAL. J. Exp. Med. **200:**1001–1013. http://dx.doi.org/10.1084/jem.20041213.
43. **Gilfillan AM, Rivera J.** 2009. The tyrosine kinase network regulating mast cell activation. Immunol. Rev. **228:**149–169. http://dx.doi.org/10.1111/j.1600-065X.2008.00742.x.
44. **Huang C, Jacobson K, Schaller MD.** 2004. MAP kinases and cell migration. J. Cell Sci. **117:**4619–4628. http://dx.doi.org/10.1242/jcs.01481.
45. **Nocka KH, Levine BA, Ko JL, Burch PM, Landgraf BE, Segal R, Lobell R.** 1997. Increased growth promoting but not mast cell degranulation potential of a covalent dimer of c-Kit ligand. Blood **90:**3874–3883.
46. **Heneberg P, Dráber P.** 2002. Nonreceptor protein tyrosine and lipid phosphatases in type I Fcε receptor-mediated activation of mast cells and basophils. Int. Arch. Allergy Immunol. **128:**253–263. http://dx.doi.org/10.1159/000063864.
47. **Hernandez-Hansen V, Smith AJ, Surviladze Z, Chigaev A, Mazel T, Kalesnikoff J, Lowell CA, Krystal G, Sklar LA, Wilson BS, Oliver JM.** 2004. Dysregulated FcεRI signaling and altered Fyn and SHIP activities in Lyn-deficient mast cells. J. Immunol. **173:**100–112. http://dx.doi.org/10.4049/jimmunol.173.1.100.
48. **Huber M, Helgason CD, Damen JE, Liu L, Humphries RK, Krystal G.** 1998. The src homology 2-containing inositol phosphatase (SHIP) is the gatekeeper of mast cell degranulation. Proc. Natl. Acad. Sci. U. S. A. **95:**11330–11335. http://dx.doi.org/10.1073/pnas.95.19.11330.
49. **Gilfillan AM, Tkaczyk C.** 2006. Integrated signalling pathways for mast-cell activation. Nat. Rev. Immunol. **6:**218–230. http://dx.doi.org/10.1038/nri1782.
50. **Iwaki S, Tkaczyk C, Satterthwaite AB, Halcomb K, Beaven MA, Metcalfe DD, Gilfillan AM.** 2005. Btk plays a crucial role in the amplification of FcεRI-mediated mast cell activation by kit. J. Biol. Chem. **280:**40261–40270. http://dx.doi.org/10.1074/jbc.M506063200.
51. **Iwaki S, Spicka J, Tkaczyk C, Jensen BM, Furumoto Y, Charles N, Kovarova M, Rivera J, Horejsi V, Metcalfe DD, Gilfillan AM.** 2008. Kit- and FcεRI-induced differential phosphorylation of the transmembrane adaptor molecule NTAL/LAB/LAT2 allows flexibility in its scaffolding function in mast cells. Cell. Signal. **20:**195–205. http://dx.doi.org/10.1016/j.cellsig.2007.10.013.
52. **Halova I, Draberova L, Draber P.** 2012. Mast cell chemotaxis—chemoattractants and signaling pathways. Front. Immunol. **3:**119. http://dx.doi.org/10.3389/fimmu.2012.00119.
53. **Pullen NA, Barnstein BO, Falanga YT, Wang Z, Suzuki R, Tamang TD, Khurana MC, Harry EA, Draber P, Bunting KD, Mizuno K, Wilson BS, Ryan JJ.** 2012. Novel mechanism for FcεRI-mediated signal transducer and activator of transcription 5 (STAT5) tyrosine phosphorylation and the selective influence of STAT5B over mast cell cytokine production. J. Biol. Chem. **287:**2045–2054. http://dx.doi.org/10.1074/jbc.M111.311142.
54. **Grange M, Verdeil G, Arnoux F, Griffon A, Spicuglia S, Maurizio J, Buferne M, Schmitt-Verhulst AM, Auphan-Anezin N.** 2013. Active STAT5 regulates T-bet and eomesodermin expression in CD8 T cells and imprints a T-bet-dependent Tc1 program with repressed IL-6/TGF-beta1 signaling. J. Immunol. **191:**3712–3724. http://dx.doi.org/10.4049/jimmunol.1300319.
55. **Pullen NA, Falanga YT, Morales JK, Ryan JJ.** 2012. The Fyn-STAT5

pathway: a new frontier in IgE- and IgG-mediated mast cell signaling. Front. Immunol. **3:**117. http://dx.doi.org/10.3389/fimmu.2012.00117.
56. **Huber M, Helgason CD, Scheid MP, Duronio V, Humphries RK, Krystal G.** 1998. Targeted disruption of SHIP leads to Steel factor-induced degranulation of mast cells. EMBO J. **17:**7311–7319. http://dx.doi.org/10.1093/emboj/17.24.7311.
57. **Deakin NO, Turner CE.** 2008. Paxillin comes of age. J. Cell Sci. **121:**2435–2444. http://dx.doi.org/10.1242/jcs.018044.
58. **Fang X, Lang Y, Wang Y, Mo W, Wei H, Xie J, Yu M.** 2012. Shp2 activates Fyn and Ras to regulate RBL-2H3 mast cell activation following FcεRI aggregation. PLoS One **7:**e40566. http://dx.doi.org/10.1371/journal.pone.0040566.
59. **Broad LM, Braun FJ, Lievremont JP, Bird GS, Kurosaki T, Putney JW, Jr.** 2001. Role of the phospholipase C-inositol 1,4,5-trisphosphate pathway in calcium release-activated calcium current and capacitative calcium entry. J. Biol. Chem. **276:**15945–15952. http://dx.doi.org/10.1074/jbc.M011571200.
60. **Litjens T, Nguyen T, Castro J, Aromataris EC, Jones L, Barritt GJ, Rychkov GY.** 2007. Phospholipase C-γ1 is required for the activation of store-operated Ca^{2+} channels in liver cells. Biochem. J. **405:**269–276. http://dx.doi.org/10.1042/BJ20061762.
61. **Antigny F, Jousset H, Konig S, Frieden M.** 2011. Thapsigargin activates Ca^{2+} entry both by store-dependent, STIM1/Orai1-mediated, and store-independent, TRPC3/PLC/PKC-mediated pathways in human endothelial cells. Cell Calcium **49:**115–127. http://dx.doi.org/10.1016/j.ceca.2010.12.001.
62. **Baba Y, Nishida K, Fujii Y, Hirano T, Hikida M, Kurosaki T.** 2008. Essential function for the calcium sensor STIM1 in mast cell activation and anaphylactic responses. Nat. Immunol. **9:**81–88. http://dx.doi.org/10.1038/ni1546.
63. **Hájková Z, Bugajev V, Dráberová E, Vinopal S, Dráberová L, Janáček J, Dráber P, Dráber P.** 2011. STIM1-directed reorganization of microtubules in activated mast cells. J. Immunol. **186:**913–923. http://dx.doi.org/10.4049/jimmunol.1002074.
64. **Chung SC, Limnander A, Kurosaki T, Weiss A, Korenbrot JI.** 2007. Coupling Ca^{2+} store release to Icrac channel activation in B lymphocytes requires the activity of Lyn and Syk kinases. J. Cell Biol. **177:**317–328. http://dx.doi.org/10.1083/jcb.200702050.
65. **Timokhina I, Kissel H, Stella G, Besmer P.** 1998. Kit signaling through PI 3-kinase and Src kinase pathways: an essential role for Rac1 and JNK activation in mast cell proliferation. EMBO J. **17:**6250–6262. http://dx.doi.org/10.1093/emboj/17.21.6250.
66. **Linnekin D, DeBerry CS, Mou S.** 1997. Lyn associates with the juxtamembrane region of c-Kit and is activated by stem cell factor in hematopoietic cell lines and normal progenitor cells. J. Biol. Chem. **272:**27450–27455. http://dx.doi.org/10.1074/jbc.272.43.27450.
67. **Lennartsson J, Ronnstrand L.** 2012. Stem cell factor receptor/c-Kit: from basic science to clinical implications. Physiol. Rev. **92:**1619–1649. http://dx.doi.org/10.1152/physrev.00046.2011.
68. **Barnstein BO, Li G, Wang Z, Kennedy S, Chalfant C, Nakajima H, Bunting KD, Ryan JJ.** 2006. Stat5 expression is required for IgE-mediated mast cell function. J. Immunol. **177:**3421–3426. http://dx.doi.org/10.4049/jimmunol.177.5.3421.
69. **Morales JK, Falanga YT, Depcrynski A, Fernando J, Ryan JJ.** 2010. Mast cell homeostasis and the JAK-STAT pathway. Genes Immun. **11:**599–608. http://dx.doi.org/10.1038/gene.2010.35.
70. **Hálová I, Dráberová L, Bambousková M, Machyna M, Stegurová L, Smrž D, Dráber P.** 2013. Crosstalk between tetraspanin CD9 and transmembrane adaptor protein non-T cell activation linker (NTAL) in mast cell activation and chemotaxis. J. Biol. Chem. **288:**9801–9814. http://dx.doi.org/10.1074/jbc.M112.449231.
71. **Samayawardhena LA, Hu J, Stein PL, Craig AW.** 2006. Fyn kinase acts upstream of Shp2 and p38 mitogen-activated protein kinase to promote chemotaxis of mast cells towards stem cell factor. Cell. Signal. **18:**1447–1454. http://dx.doi.org/10.1016/j.cellsig.2005.11.005.
72. **Samayawardhena LA, Kapur R, Craig AW.** 2007. Involvement of Fyn kinase in Kit and integrin-mediated Rac activation, cytoskeletal reorganization, and chemotaxis of mast cells. Blood **109:**3679–3686. http://dx.doi.org/10.1182/blood-2006-11-057315.
73. **Metcalfe DD, Baram D, Mekori YA.** 1997. Mast cells. Physiol. Rev. **77:**1033–1079.
74. **Williams CM, Galli SJ.** 2000. The diverse potential effector and immunoregulatory roles of mast cells in allergic disease. J. Allergy Clin. Immunol. **105:**847–859. http://dx.doi.org/10.1067/mai.2000.106485.
75. **Schuck S, Honsho M, Ekroos K, Shevchenko A, Simons K.** 2003. Resistance of cell membranes to different detergents. Proc. Natl. Acad. Sci. U. S. A. **100:**5795–5800. http://dx.doi.org/10.1073/pnas.0631579100.
76. **Garner AE, Smith DA, Hooper NM.** 2008. Visualization of detergent solubilization of membranes: implications for the isolation of rafts. Biophys. J. **94:**1326–1340. http://dx.doi.org/10.1529/biophysj.107.114108.